POLITECNICO DI MILANO
Scuola di Ingegneria dei Processi Industriali

Corso di Laurea Specialistica in Ingegneria Nucleare

FEASIBILITY STUDY OF A NEUTRON SPECTROMETER FOR COMPLEX FIELDS

Relatore:
Prof. Andrea POLA

Correlatore:
Dott. Roberto BEDOGNI

Tesi di Laurea di:
Davide BORTOT
Matr. 745880

Anno Accademico 2011-2012

CONTENTS

LIST OF FIGURES

LIST OF TABLES

ABSTRACT

The Italian National Institute for Nuclear Physics (INFN), the Politecnico di Milano and the Centro de Investigaciones Energéticas, Medioambientales y Tecnológicas (CIEMAT) of Madrid proposed in 2011 the experiment NEutron Spectrometry in COmplex FIelds @ Beam Test Facility (NESCOFI@BTF). This experiment aims at developing innovative neutron sensitive instruments for the spectrometric and dosimetric characterization of neutron fields intentionally produced or present as parasitic effects in particle accelerators employed for industrial, research and medical applications. More specifically, the project goal is the development of two types of real-time spectrometers for different neutron field geometries: a cylindrical spectrometer, meant for collimated neutron beams, and a spherical one, aimed at measuring the neutron fluence spectrum independently from its direction distribution. Both of them will be constituted of a single moderator embedding several *direct reading* thermal neutron detectors at different positions. This master Thesis discusses the preliminary study carried out for identifying innovative active sensors able to detect thermal neutrons with an adequate sensibility (defined as the ratio of the number of counts to the incident thermal neutron fluence) and, at the same time, small, cheap, robust and easy-to-multiply. It should be underline that, at present, the design and the fabrication process of the sensors are patent pending.

The first part of the present master Thesis describes the study and the development of suitable active sensors to be used in the spectrometers proposed in the framework of the NESCOFI@BTF Project. A dedicated Data AcQuisition system for the pre-filtering and the acquisition of signals generated by the Active Thermal Neutron Detectors (ATND) and a custom user interface based on the Labview2010© software for the digital filtering and signal processing in streaming mode were developed. Test irradiations with thermal neutrons demonstrated a neutron response equal to 0.021 cm^2. Preliminary irradiations of a low-cost prototype of the cylindrical spectrometer, equipped

with the previously developed active sensors, confirmed the possibility of simultaneously acquire and elaborate signals from different active thermal neutron detectors within a single moderating structure, but also pointed out some criticalities to face, regarding both the discrete acquisition electronics and the neutron response of the active sensors.

In order to overcome these critical aspects, new solutions were proposed. A multiple discrete electronic chains were integrated and parallelized in portable multi-channel boards and another type of active thermal neutron detector was developed.

Finally, the two types of ATND were tested within a standard Extended Range Bonner Sphere Spectrometer System (ERBSS), in order to check their performances for neutron spectrometry. Preliminary data demonstrated the agreement between results derived through the new sensors with respect to a reference ^{6}LiI ATND.

ESTRATTO

Questo lavoro di tesi è stato svolto nell'ambito del progetto NEutron Spectrometry in COmplex FIelds @ Beam Test Facility (NESCOFI@BTF) dell'Istituto Nazionale di Fisica Nucleare (INFN), in collaborazione con il Politecnico di Milano e il Centro de Investigaciones Energéticas, Medioambientales y Tecnológicas (CIEMAT) di Madrid. NESCOFI@BTF mira allo sviluppo di tecniche innovative per la caratterizzazione spettrometrica e dosimetrica di fasci di neutroni prodotti intenzionalmente o presenti come effetto secondario presso acceleratori ad uso industriale, medico o di ricerca. Tali fasci spaziano da energie termiche sino alle centinaia di MeV, presentano ratei di fluenza variabili da poche decine fino a 10^5 n cm^{-2} s^{-1} e possono avere una struttura pulsata.

Attualmente lo spettrometro a Sfere di Bonner è l'unico strumento universalmente riconosciuto e ampiamente validato per la determinazione di tutte le componenti energetiche del campo neutronico. Tale rivelatore, tuttavia, non è adatto per il monitoraggio in continuo del fascio, in quanto richiede l'esposizione sequenziale, nello stesso punto di misura, di almeno dieci sfere moderatrici di diverso diametro.

Il progetto NESCOFI@BTF prevede la realizzazione di tre spettrometri di tipo *monitor-unit* in grado di fornire lo spettro neutronico in un unico irraggiamento, permettendo così di monitorare eventuali deviazioni rispetto alle caratteristiche nominali del fascio ed eventuali perturbazioni che gli oggetti irraggiati, o i pazienti trattati, possono indurre sul fascio stesso. L'idea di base consiste nell'utilizzo di un singolo materiale moderante contenente diversi rivelatori attivi per neutroni termici posti in varie posizioni al suo interno. Più specificamente, si intende sviluppare due tipologie di spettrometro, a seconda delle caratteristiche del fascio neutronico in oggetto:

- uno spettrometro cilindrico (CYSP), dedicato a fasci neutronici collimati o alla determinazione dello spettro del contributo neutronico proveniente da una determinata direzione, eliminando così tutte le altre componenti;

- due spettrometri sferici $(SP)^2$, adatti per la misura dello spettro in fluenza indipendentemente dalla direzione del fascio: il primo, denominato Low-energy SP^2, per neutroni con energie fino a 20 MeV; il secondo, detto High-energy SP^2, per energie neutroniche fino a centinaia di MeV.

In entrambi i casi, le distribuzioni energetica e spaziale del campo neutronico verrebbero ricavate tramite appositi algoritmi di unfolding, in base alla matrice risposta del sistema e ai conteggi ottenuti dai vari rivelatori.

Per quanto concerne i due spettrometri sferici, una vasta campagna di simulazioni, eseguita nel corso del 2011, ha portato ad identificare la dimensione appropriata dei moderatori e la disposizione dei rivelatori di neutroni termici al loro interno:

- il prototipo Low-energy consiste in una sfera di polietilene di 30 cm di diametro, dotata di 37 posizioni di misura lungo i tre assi;
- la versione High-energy è costituita da una sfera di polietilene con diametro di 25 cm e 31 posizioni di misura lungo i tre assi. Essa include, inoltre, un degradatore in piombo spesso 1 cm con diametro interno di 3.5 cm, con lo scopo di promuovere reazioni (n, xn), estendendo l'intervallo di risposta in energia sino a centinaia di MeV.

Entrambe le versioni Low-energy e High-energy sono state fabbricate e testate in campi neutronici con distribuzione energetica nota, con lo scopo di confermare sperimentalmente la matrice risposta del sistema precedentemente determinata tramite simulazioni Monte Carlo.

Per quanto riguarda lo spettrometro cilindrico (CYSP), è tuttora in atto una campagna di simulazione volta ad identificare la dimensione definitiva del moderatore, il numero e la distribuzione dei rivelatori attivi, la tipologia più idonea di collimatore per sopprimere le componenti provenienti da direzioni diverse rispetto a quella del fascio primario, e le caratteristiche del materiale da utilizzare come degradatore per neutroni di alta energia. Per il momento è stato sviluppato un prototipo semplificato a basso costo,

denominato Mini-Cysp, con lo scopo di effettuare alcuni irraggiamenti preliminari: esso è costituito da un cilindro di polietilene con sette cavità interne in cui alloggiare i rivelatori attivi.

La prima parte di questo lavoro di Tesi ha riguardato lo studio e lo sviluppo di appositi rivelatori attivi per neutroni termici da inserire all'interno degli spettrometri finali proposti nell'ambito del progetto NESCOFI@BTF, nonché del sistema di acquisizione digitale del segnale generato dagli stessi.

La scelta del sensore ottimale si è basata principalmente su tre aspetti imprescindibili, dati dalla riposta ai neutroni (definita come numero di conteggi su unità di fluenza termica incidente), dalle dimensioni e dal costo: l'area massima disponibile nelle varie cavità degli spettrometri è pari a 1.5×1.5 cm^2, e il costo unitario deve essere adeguato, considerando il grande numero di rivelatori necessari (37 nello spettrometro Low-energy SP^2, 31 in quello High-energy SP^2 e approssimativamente 8 nello spettrometro CYSP). E' importante precisare che tutte le informazioni relative alla progettazione e alla fabbricazione di suddetti rivelatori, denominati D1, sono attualmente riservate, in quanto in fase di brevettazione.

L'acquisizione dei segnali generati dai rivelatori è basata su una tecnica digitale. Prevedendo la necessità di acquisire e processare dati provenienti da molti sensori, è stato selezionato un oscilloscopio digitale commerciale, modello NI USB-6366, il quale fornisce otto ingressi analogici campionati con una frequenza massima di 2 MS s^{-1} e una risoluzione di 16 bits. Il segnale in uscita dal digitalizzatore viene poi elaborato tramite un programma Labview2010 interamente sviluppato nell'ambito di questo lavoro di Tesi, costituito da quattro differenti pannelli: il primo contiene le impostazioni di acquisizione, quali il numero di canali attivi (da un minimo di uno a un massimo di otto), il livello del trigger, la dinamica, la frequenza di campionamento e la dimensione del buffer; gli altri tre mostrano, in tempo reale e per ogni canale attivo, i grafici dell'andamento del segnale nel tempo, gli spettri di altezza di impulso ottenuti tramite una funzione di ricerca picchi nel segnale di ingresso, e i grafici relativi al rateo di conteggi a intervalli temporali di un secondo, rispettivamente. Al termine di ogni misura, gli spettri relativi ai canali attivi, nonché il valore dei parametri di acquisizione impostati nel primo pannello, vengono salvati su file, per poter essere elaborati a posteriori.

Test preliminari in campi neutronici generati da una sorgente di calibrazione di Am-Be hanno dimostrato una risposta massima ai neutroni termici del sensore D1 pari a circa 0.021 cm^2. I rivelatori sviluppati sono stati successivamente provati all'interno del Mini-Cysp, il prototipo semplificato dello spettrometro cilindrico descritto precedentemente. Esso è costituito da un cilindro di polietilene di 40 cm di diametro e 50 cm di altezza, ed è dotato di 7 posizioni di misura nelle quali sono stati alloggiati i sensori. Il prototipo è stato irraggiato con neutroni monoenergetici da 5 MeV e 565 keV. I segnali analogici generati dai rivelatori sono stati processati mediante 4 catene elettroniche indipendenti, costituite da moduli commerciali di preamplificatori di carica e amplificatori formatori. Gli impulsi analogici in uscita dai formatori sono stati digitalizzati tramite l'oscilloscopio NI USB-6366, mentre l'elaborazione dei dati è stata effettata con il programma di acquisizione precedentemente descritto. Tali misure hanno confermato la possibilità di acquisire ed elaborare segnali generati da diversi sensori attivi inseriti nella medesima struttura moderante, ma hanno evidenziato, al contempo, alcuni aspetti critici riguardanti sia l'utilizzo di un'elettronica discreta sia la risposta dei rivelatori ai neutroni. La gestione di quattro catene analogiche, inserite in otto diversi contenitori (quattro per i preamplificatori di carica e altri quattro per gli amplificatori formatori) si è rivelata poco agevole, non solo per semplici motivi di spazio, ma anche in riferimento alla localizzazione e alla rimozione di sorgenti di rumore estrinseco, quali i giri di massa. Per questi motivi, e in previsione dello sviluppo degli spettrometri finali, le singole catene elettroniche discrete sono state integrate in schede compatte portatili da 2 e da 8 canali.

Per quanto riguarda il secondo aspetto critico, la discriminazione tra segnali neutronici e gamma negli spettri di altezza di impulso è risultata alquanto complessa, poiché i rispettivi contributi risultavano sovrapposti in alcune aree dello spettro. Ciò ha inevitabilmente portato a scartare un grande numero di conteggi per poter assicurare la selezione del solo contributo neutronico, riducendo l'efficienza finale ad un valore notevolmente più basso rispetto a quello previsto teoricamente. L'ampiezza dei segnali dovuti ai neutroni termici, inoltre, era molto prossima al valore di soglia di acquisizione: anche un esiguo aumento del rumore elettronico associato al sistema o la presenza di una sorgente di interferenza, necessariamente influirebbe sul risultato della misura.

Per poter risolvere queste due problematiche, si è deciso di sviluppare un ulteriore tipo di rivelatore attivo, denominato D2, tenendo sempre in considerazione i medesimi requisiti riguardanti la risposta ai neutroni, la dimensione e il costo. Tutti i dati relativi a questo secondo tipo di sensore e le fasi del suo sviluppo saranno omessi, perché in fase di brevettazione.

Irradiazioni con neutroni termici effettuate con il medesimo apparato sperimentale utilizzato nella caratterizzazione dei rivelatore D1, hanno dimostrato una sensibilità ai neutroni del sensore D2 pari a circa 0.026 cm^2. Dai risultati emersi e dal confronto complessivo tra le prestazioni dei due diversi rivelatori, è stato possibile concludere che la loro risposta è molto simile, tuttavia il secondo sensore permette una discriminazione n-γ molto più efficace e semplice da implementare..

Infine i sensori D1 e D2 sono stati utilizzati all'interno di moderatori di riferimento facenti parte di uno Spettrometro a sfere di Bonner a risposta estesa (ERBSS), con il fine di verificare le loro prestazioni in misure di spettrometria neutronica. Il campo neutronico, indotto da un fascio di protoni da 30 MeV su un target di berillio, è stato generato tramite il ciclotrone Gustaf Werner presso i Laboratori Svedesi dell'Università di Uppsala. Poiché i dati di riferimento associati agli irraggiamenti, in particolare la corrente del fascio di protoni e le fluenze neutroniche, non sono ancora disponibili, i risultati sperimentali si riferiscono al valore nominale della corrente di protoni.

Sono state esposte al campo neutronico otto sfere di Bonner standard ed una a risposta estesa, munita di attenuatore di piombo, al centro delle quali sono stati impiegati tre diversi rivelatori: uno scintillatore cilindrico a ioduro di litio-6 (^{6}LiI), utilizzato come riferimento, un rivelatore D1 e un rivelatore D2.

Nonostante i dati di riferimento non siano ancora pervenuti, un'analisi preliminare, basata sul valore nominale delle correnti di protoni, conferma che tali rapporti variano di circa il 4.0 % per D1 e il 3.2 % per D2, al variare della sfera. Una caratterizzazione più dettagliata sarà eseguita non appena i dati effettivi saranno disponibili. L'efficienza dei sensori D1 e D2 è risultata circa otto volte più bassa rispetto a quella del sensore ^{6}LiI. D'altro canto, il grande vantaggio di questi nuovi rivelatori, se paragonati allo scintillatore, consiste nelle loro dimensioni ridotte e nel loro basso costo.

In conclusione, è possibile affermare che i rivelatori attivi di neutroni termici da inserire all'interno degli spettrometri finali, proposti nell'ambito del progetto NESCOFI@BTF, saranno costituiti da sensori di tipo D2.

INTRODUCTION

A large interest has gradually arisen and currently exists for on-line neutron spectrometry that would allow to estimate field perturbations due to irradiated objects, to evaluate the importance of room-return for different user positions, and to prevent beam alterations due to any change in energy or space characteristics of the primary beam. Moreover, the medical physics community is seeking on-line instruments able to measure proper quantities for in-phantom or in-vivo characterizations where an accurate knowledge of the neutron spectrum over a wide energy range is required.

The present Master's thesis work originates from the NEutron Spectrometry in COmplex FIelds @ Beam Test Facility (NESCOFI@BTF) Project of the Italian National Institute for Nuclear Physics (INFN), in collaboration with Politecnico di Milano and Centro de Investigaciones Energéticas, Medioambientales y Tecnológicas (CIEMAT) of Madrid. The basic idea behind the project is to exploit the moderation of neutrons in hydrogenated materials, but with new detection systems and computational methods. In particular, the measurement of neutron energy distribution with a single moderator embedding several "direct reading" thermal neutron detectors at different positions is proposed as an effective alternative to the standard multi-spheres approach.

In chapter 1 the main exploited reactions in slow neutron detection methods are described. Some information regarding the Bonner Sphere Spectrometer technique are also reported.
Chapter 2 illustrates the main purpose of the NESCOFI@BTF Project and summarizes the experimental activities carried out in 2011.
Chapter 3 describes the study and the development of suitable *direct reading* thermal neutron detectors to be used in the spectrometers proposed in the framework of the NESCOFI@BTF Project. Moreover the Data AcQuisition system for the processing and

acquisition of signals generated by the Active Thermal Neutron Detectors (ATND) is discussed. A dedicated Labview2010 program, whose purpose is to simultaneously acquire and process pulses provided by eight different detectors, is explained.

Some irradiation tests of a low-cost prototype of the Cylindrical Spectrometer equipped with the previously developed active sensors are described in chapter 4. These measurements pointed out some criticalities to face, regarding both the discrete acquisition electronics and the neutron response of the active sensors.

In chapter 5, new electronic integrated boards are described and the development of another type of active thermal neutron detector is explained. Performances of the two ATND are finally compared.

In chapter 6, an application of the developed ATND in neutron spectrometry measurements with the Bonner Sphere Spectrometer is presented.

It should be underlined that all information concerning the ATND design and fabrication are patent pending.

1

NEUTRON PHYSICS

1.1 Introduction

Neutrons, together with protons, play a fundamental role in the study of nuclear forces and of the atomic nucleus formation[1]. Their existence was predicted by Ernest Rutherford in 1920, but the first experimental evidence came ten years after, when Walther Bothe and Herbert Becker bombarded beryllium with α particles from a ^{210}Po radioactive source[2]. They observed the emission of a very penetrating but non-ionizing radiation, which they assumed to be high-energy photons. Around 1931, Irène Joliot-Curie and Fréderic Joliot noticed that, when this radiation hit a paraffin target, energetic protons with an energy of 5.3 MeV were emitted. They estimated, using the Compton scattering formula, that the photons originating such protons would necessarily have an energy of at least 52 MeV, which seemed extremely unlikely at that time. One year later, James Chadwick repeated the same experiment with other recoil nuclei and he provided the correct explanation, identifying the unknown radiation as electrically neutral with nearly the same mass as that of the proton and naming it *neutron*.

Neutrons interact through strong nuclear forces, have a rest mass of 939.573 MeV c^{-2} - slightly larger than that of protons -, no net electric charge and spin 1/2. However, the inner distribution of positive and negative charges gives rise to electromagnetic momenta. Extremely weak electromagnetic forces may appear when these momenta are coupled with the charge and spin of atomic orbital electrons. Therefore, neutrons can travel considerable distances in matter until either a collision or an interaction with a nearby nucleus takes place due to nuclear forces leading to scattering or capture processes[3]. Neutrons are generally stable when they are well bounded within the atomic nucleus,

while free neutrons outside the atomic nucleus decay into a proton, an electron and an electron antineutrino with a half-life of about 10.6 min.

The probability that an interaction takes place between an incident neutron and a target nucleus is expressed through the concept of the microscopic cross section (σ), which has the dimensions of an area and is commonly expressed in barns (1 b = 10^{-24}cm^2). Considering a large number of neutrons of the same energy directed towards a given material layer, three different situations are possible: i) some of them may pass through the material with no interactions, ii) others may have interactions that change their directions and energies, and iii) others may be captured. Neutrons can be detected by exploiting the secondary charged particles generated by their interactions in a given material.

1.2 Neutron detection methods

Neutrons are classified on the basis of their kinetic energy E_n:

- *High-energy* if $E_n > 100$ MeV
- *Fast* if 100 keV $< E_n <$ 100 MeV
- *Epithermal* if 0.1 eV $< E_n <$ 100 keV
- *Thermal* if $E_n <$ 0.1 eV

Neutrons with energies above 10 MeV interact mainly through inelastic scattering (n, n$^/$) with high Z materials and are able to induce spallation reactions like (n, xn) or (n, np).

In the energy range between 10 MeV and 100 keV, neutrons can undergo elastic scattering (n, n) with low Z materials like hydrogen, carbon and oxygen, transferring part of their energy to the recoil nuclei. Inelastic interactions are still important at the higher energies or for high *Z* materials .

Neutrons may slow down through multiple elastic collisions with the nuclei of the medium, becoming epithermal neutrons with an energy distribution proportional to $1/E_n$.

In this energy range, neutron resonance processes, due mainly to (n, γ), (n, p), (n, α) and (n, fission) reactions, become important.

Below 0.1 eV, neutrons reach thermal equilibrium with the surrounding atoms or molecules of the medium, exhibiting a Maxwellian energy distribution. The most probable energy for thermal neutrons is given by:

$$E_0 = k_B * T \tag{1.1}$$

where k_B is the Boltzmann constant and T is the medium absolute temperature.

At a room temperature (20°C), the most probable energy for thermal neutrons is $E_0 \sim 0.0253\ eV$.

For most stable elements, neutron absorption takes place through radiative capture (n, γ) reactions, but nuclear reactions like (n, p) or (n, α) are also possible for some low Z nuclei. The relative probabilities of the different types of neutron interactions with matter change with neutron energy. In general, neutrons are classified in two categories depending on their energy: they are considered either *fast* neutrons or *slow* neutrons, where the conventional threshold corresponds to the energy of the abrupt drop in cadmium absorption cross section (the so called *cadmium cutoff energy*).

The slow neutron interactions exploited in neutron detection methods are nuclear reactions that can generate secondary radiation of energy sufficiently high to be directly detected. Reactions such as (n, α), (n, p) and (n, fission) are exploited, as the secondary radiations are charged particles that can be easily detected. For this reason, neutron detectors consist generally in a combination of a target material suitable for the conversion and a conventional detector for the reaction products.

In order to exploit nuclear reactions for slow neutron detection, two essential factors must be considered: a) microscopic cross section and b) Q-value.

a) The conversion reaction cross section has to be as large as possible, in order to obtain high detection efficiencies, enabling the use of smaller detectors. For the same reason, the target nuclide should feature a high isotopic abundance in the natural element, or it should be artificially enriched with low-cost techniques.

b) The Q-value of the reaction must be high. The higher the Q-value, the greater the energy given to the reaction products, and the easier is the processing of the generated signals.

The main exploited reactions in slow neutron detection methods are described in the following.

1.2.1 The ^{10}B(n, α)^{7}Li reaction

The isotope ^{10}B is commonly used for the conversion of slow neutrons into directly detectable particles through the reaction:

$$ {}^{10}_{5}B + {}^{1}_{0}n \rightarrow \begin{cases} {}^{7}_{3}Li + {}^{4}_{2}\alpha & (6\ \%) \quad Q = 2.792\ MeV \\ {}^{7}_{3}Li^{*} + {}^{4}_{2}\alpha \rightarrow {}^{7}_{3}Li + {}^{4}_{2}\alpha + \gamma(482\ keV) & (94\ \%) \quad Q = 2.310\ MeV \end{cases} $$

where the reaction product ^{7}Li may be left either in its ground state (branching ratio of about 6 %) or in its first excited state (branching ratio of about 94 %). In either case, the Q-value is very large compared with the energy of the slow incident neutron, so that the energy of the α particle and ^{7}Li corresponds approximately to the Q-value itself.

It is possible to calculate individual energies of the two reaction products by applying the conservation of energy and momentum as follows:

$$ \begin{cases} E_{Li} + E_{\alpha} = Q \\ m_{Li} v_{Li} = m_{\alpha} v_{\alpha} \end{cases} \tag{1.2} $$

In the case of the excited state of ^{7}Li, E_{Li} and E_{α} are equal to 0.84 MeV and 1.47 MeV respectively, while for reactions leading to the ground state the corresponding values are about 1.02 MeV and 1.78 MeV respectively.

The thermal neutron cross section for this reaction is about 3840 b. This value rapidly decreases with increasing neutron energy, being proportional to *1/v*, where *v* is the neutron velocity (Figure 1.1).

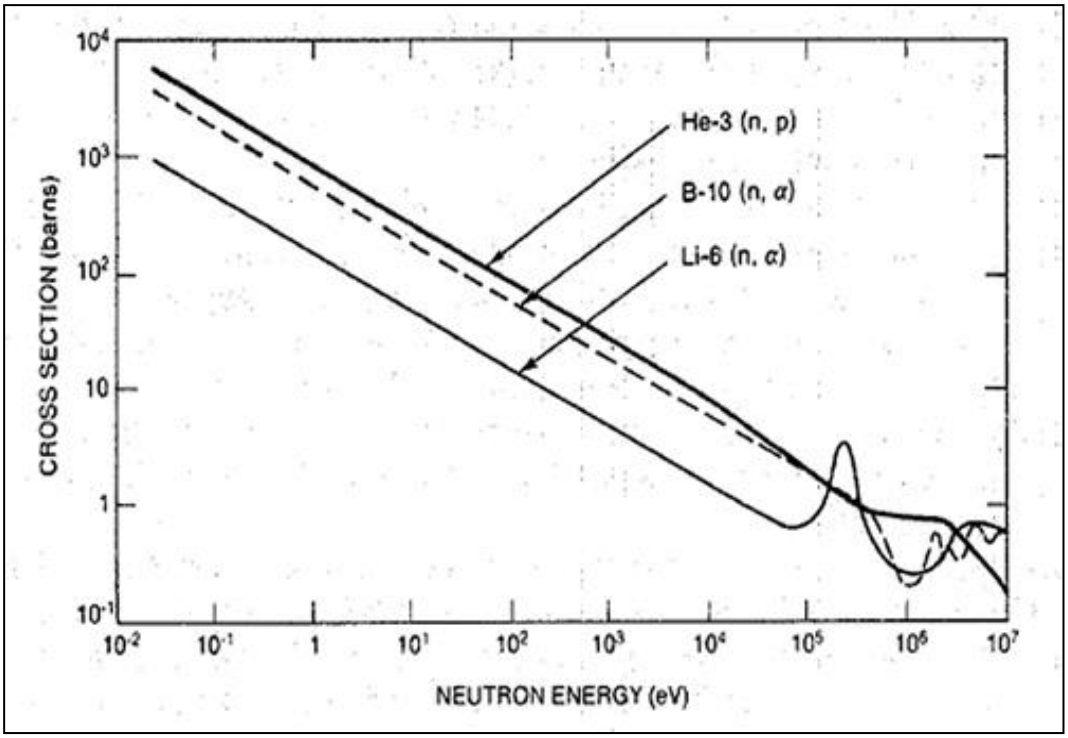

Figure 1.1: Cross sections as a function of neutron energy for $^{10}B(n, \alpha)^{7}Li$, $^{6}Li(n, \alpha)^{3}H$ and $^{3}He(n, p)^{3}H$ reactions[4].

The natural isotopic abundance of ^{10}B is 19.8 %, but for neutron detection purposes materials enriched in ^{10}B up to 95 % are employed, in order to increase the intrinsic efficiency.

Boron can be used both in the form of a solid coating on the interior walls of a conventional proportional counter, and in the form of BF_3 gas: in the latter case, BF_3 serves both as a target for slow neutrons as well as a proportional gas. In almost all detectors, the gas is highly enriched in ^{10}B, resulting in an efficiency about five times greater than that of natural boron.

1.2.2 The $^{6}Li(n, \alpha)^{3}H$ reaction

This reaction leads only to the ground state of ^{3}H:

$$^{6}_{3}Li + ^{1}_{0}n \rightarrow ^{3}_{1}H + ^{4}_{2}\alpha \qquad Q = 4.78\ MeV$$

where, for negligible incident neutron energy, E_H and E_α are equal to 2.73 MeV and 2.05 MeV, respectively. Reaction products are emitted in opposite directions when the incoming neutron energy is low. The cross section for this reaction is about 940 barns for thermal neutrons, but it shows a resonance for neutron energies between 100 keV and 500 keV (see Figure 1.1).

For this reaction no nuclear de-excitation gamma rays are emitted. This fact can be an advantage for detection purposes, together with the higher energy of reaction products with respect to the ^{10}B(n, α)^{7}Li reaction, even if the cross section is lower.

1.2.3 The ^{3}He(n, p)^{3}H reaction

The ^{3}He gas is used as a detection medium for neutrons when the following reaction occurs:

$$^{3}_{2}He + ^{1}_{0}n \rightarrow ^{3}_{1}H + ^{1}_{1}p \qquad Q = 0.764\ MeV$$

where, for thermal incident neutrons, E_p = 573 keV and E_H = 191 keV.

The thermal neutron cross section is 5330 barns, higher than that for ^{10}B and ^{6}Li reactions (see Figure 1.1).

^{3}He is a noble gas, and therefore no solid compounds can be fabricated and the material must be used in gaseous form, inside ionization chambers and proportional counters.

1.2.4 Neutron-induced fission reactions

Materials like ^{233}U, ^{235}U and ^{239}Pu can be used in slow neutron detectors thanks to their relatively large fission cross section. ^{235}U fission reaction is expressed as:

$$^{235}_{92}U + ^{1}_{0}n \rightarrow ^{A}_{Z}FF_1 + ^{A}_{Z}FF_2 + 2.47\ n \qquad Q = 0.764\ MeV$$

where FF_1 and FF_2 indicate two different fission fragments. The Q-value is equal to 207 MeV, which is extremely large compared with those of the previous reactions. The total energy produced in this reaction is distributed to both neutrons and fission products;

in particular, about 168 MeV appears as kinetic energy of the two fragments. As a result, detectors based on the fission reaction can often give output pulses that are much larger than those induced from other reactions or incident gamma rays.

Almost all fissile nuclides are naturally alpha-emitters. As a consequence, detectors containing these materials show also an output signal due to alpha particles, whose energy, however, is lower than the energy released in a fission reaction. For this reason, it is sufficient to insert an appropriate threshold in the acquisition system to discard the alpha contribution.

The most popular form of fission detector is an ionization chamber with its inner surfaces coated with a fissile material.

1.2.5 Radiative capture reactions (n, γ)

Radiative capture reactions are generally exploited to detect thermal and epithermal neutrons due to their large thermal cross section. Neutron measurements are carried out by measuring the radioactivity induced in some materials by neutron interactions. More in detail, a sample is exposed to a neutron flux and then removed. Afterwards, the induced radioactivity is counted generally by employing a Geiger detector for β^- particles and a scintillator or a germanium detector for γ rays emitted during the decay. In order to achieve a high sensitivity, these activation materials must have large cross sections for a neutron-induced reaction, and their thickness has to be kept small not to perturb the neutron flux.

Corrections have to be applied in order to take into account the irradiation time, the post-irradiation delay, and the measurement time. The most widely used capture reactions are:

$^{197}_{79}Au(n,\gamma)^{198}_{79}Au \qquad \sigma_{th} = 98.8\ barns$

$^{115}_{49}In(n,\gamma)^{116m}_{49}In \qquad \sigma_{th} = 160\ barns$

$^{164}_{66}Dy(n,\gamma)^{165}_{66}Dy \qquad \sigma_{th} = 800\ barns$

All of the isotopes produced are β-emitters, with half lives of about 2.7 days, 54.1 minutes, and 140 minutes, respectively.

1.3 Neutron spectrometry

All neutron spectrometry techniques are based on the detection of secondary radiations (*i.e.*, charged particles or photons) deriving from the interaction of neutrons with matter. Methods for neutron spectrometry can be classified into seven groups based on the principle used [5]:

1) neutron scattering and measurement of the energies of recoil nuclei;
2) measurement of the energies of charged particles released during neutron-induced nuclear reactions;
3) methods in which the neutron velocity is measured;
4) threshold methods, in which the appearance of a neutron-induced effect, such as radioactivity for instance, indicates that the neutron energy is not lower than a given value;
5) methods in which the neutron energy distribution is determined by unfolding a set of readings of several detectors that differ in the energy-dependence of their response to neutrons;
6) neutron diffraction;
7) measurement of the time-distribution of the slowdown of a short burst of high-energy neutrons in a suitable medium.

Since the discovery of neutrons by Chadwick (1932), many methods for measuring neutron energy distributions have been developed. Before 1960 the following spectrometers techniques were already in use: nuclear emulsions, proportional counters, organic scintillators and recoil telescopes[5]. ^{3}He proportional counters and ^{6}LiI(Eu) scintillators, where the energy of the charged particles produced by nuclear reactions was measured, were used as well. During the same period the time-of-flight and the activation foils techniques were also known.

A decisive development occurred in 1960 with the introduction of the multi-sphere spectrometer, also called Bonner Sphere Spectrometer (BSS), which is based on a thermal

neutron sensor placed at the centre of polyethylene spheres featuring different diameters (up to 18”). Iterative unfolding codes were introduced, allowing to infer the neutron spectrum on the basis of the readings of the different spheres.

Semiconductor-based spectrometers were introduced in 1963, and superheated drop detectors were firstly used by Apfel in 1979. Since the 80s, a considerable technological progress was achieved, but the most important improvement was the impact of computers on neutron spectrometry: Monte Carlo codes were used to generate the response functions of the detectors, and iterative algorithms were applied to unfold the neutron spectra from the spectrometer readings.

In addition to the BSS technique, several other methods are widely used at present e.g. recoil neutron spectrometers, nuclear-reaction based spectrometers, time-of-flights methods, thermoluminescent crystals and solid-state nuclear track detectors[5]. Some information of interest for this work regarding the BSS technique are reported in the following.

1.4 The Bonner Sphere Spectrometer

The Bonner Sphere Spectrometer (BSS), firstly described by Bramblett, Ewing and Bonner in 1960, consists of a thermal neutron sensor placed at the centre of a number of moderating spheres of different diameter[6]. Thermal sensors are used to detect moderated neutrons as direct fast neutron detection is complex and the related cross sections show lower values than those of thermal neutrons. These spheres are made of polyethylene $(C_2H_4)_n$. This type of spectrometer has an almost isotropic response and can cover the energy range from thermal to GeV .

The sensitivity of each sphere shows a maximum at a particular neutron energy depending on its diameter: as the size of the sphere increases, thermalisation is more effective for higher incident neutron energies and the maximum response of the sphere-detector assembly shifts towards higher energies. From the readings of a set of spheres, information can be derived about the spectrum of the neutron field.

The *response* is generally defined as the ratio of the instrument reading to the physical quantity of interest. The *fluence response* of BSS, expressed in terms of (cm^2), is defined by:

$$R_i(E) = \frac{M_i}{\Phi(E)} \tag{1.3}$$

where M_i is the reading of the sphere (counts), $\Phi(E)$ is the neutron fluence (neutrons cm^{-2}) at neutron energy E at the center of the sphere. This definition includes the requirement that the sphere must be uniformly irradiated by neutrons.

The *efficiency* of the *i*-sphere to neutrons of energy E is the ratio of the reading M_i to the number of neutrons of this energy entering the sphere. Considering a homogeneous irradiation of the sphere, the number of neutrons of energy E entering the sphere is defined by:

$$\#\,\mathrm{n}(E) = \Phi(E) * \frac{\pi {D_i}^2}{4} \tag{1.4}$$

where D_i is the sphere diameter and $\pi D_i^2/4$ is the geometrical cross section of the sphere. Then the following relationship for the efficiency is obtained:

$$\varepsilon_{\,\mathrm{i}}(E) = \frac{M_i}{\#\,\mathrm{n}(E)} = \frac{4\mathrm{R_i}(E)}{\pi {D_i}^2} \tag{1.5}$$

The main operating principle of a BSS is the moderation of neutrons within the spheres, mainly via elastic scattering with hydrogen nuclei. Neutron interactions with a Bonner Sphere can be described by different types of history.

Figure 1.2 shows an example of the response functions of a set of spheres of different sizes. The peak in the response function moves towards higher energies as the diameter of the sphere increases. The efficiency, however, decreases systematically with increasing sphere diameter.

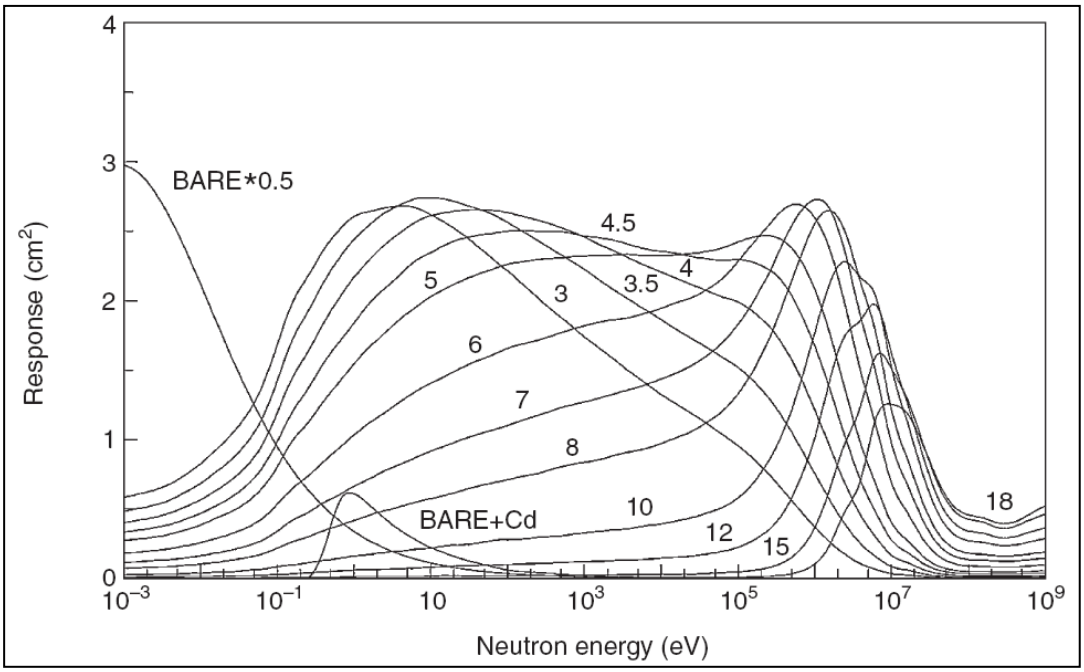

Figure 1.2: Fluence response functions of the PTB sphere spectrometer[6].

1.4.1 BBS response function

Each sphere-detector combination *i* has a unique response function $R_i(E)$, which is a continuous function of the neutron energy *E*. If this sphere is exposed in a neutron field with spectral fluence $\Phi_E(E)$, the sphere reading M_i is obtained by "folding" $R_i(E)$ with $\Phi_E(E)$:

$$\mathrm{M_i} = \int R_i(E)\,\Phi_E(E)\,dE \tag{1.6}$$

This *folding* process takes place in the sphere itself during the measurement, where the quantities $R_i(E)$ and $\Phi_E(E)$ are the true response of *i*-sphere and the true fluence spectral distribution of the investigated neutron field, respectively.

The inverse process, called *unfolding* procedure, allows to derive the neutron spectrum from the readings, provided that the corresponding response functions are well known. Although the real $\Phi_E(E)$ and $R_i(E)$ are continuous functions of neutron energy, they cannot be described by analytical functions, because of the finite number of measurements, therefore a discretised numerical form is used:

$$\mathrm{M_i} = \sum R_i(E_j)\,\Phi_E(E_j)\,\Delta E_j = \sum R_i(E_j)\;\Phi(E_j) = \sum R_{ij}\,\Phi_j \quad (j = 1, 2, \ldots, n_E) \qquad (1.7)$$

where Φ_j is the neutron fluence in the *j*th energy group of width ΔE_j centred on the energy E_j and R_{ij} is the fluence response function (calculated via Monte Carlo code or other techniques) of *i*th sphere for an energy group *j*.

The spectral information about a neutron field is thus contained in a vector $\boldsymbol{\Phi}$ with n_E energy groups Φ_j. If measurements are performed in this neutron field with a set of n_S Bonner Spheres, a set of n_S readings M_i (the components of the reading vector **M**) is obtained. A set of n_S linear equations can be written as:

$$\mathbf{M} = \boldsymbol{R}\,\boldsymbol{\Phi} \qquad (1.8)$$

where the n_S x n_E rectangular matrix **R** is the fluence response matrix of the Bonner Sphere set. If all components of the response matrix **R** are known, it should be possible to determine, using the set of n_S measured readings M_i and by applying an appropriate unfolding procedure, the n_E components of $\boldsymbol{\Phi}$.

In most cases, measurements with Bonner Spheres aim to establish the spectral neutron fluence distribution (neutron spectrum) at a given point "point of measurement". For that purpose, the measurements are performed placing the spheres, one after another, centered at the same reference point.

1.4.2 Unfolding procedures

In general, the unfolding procedure in Bonner sphere spectrometry is a typical few-channel unfolding, since the number of individual measurements, n_S, is largely smaller that the number of unknown energy groups, n_E. In addition, BSS individual measurements cannot be considered independent since the sphere response functions overlap in some neutron energy intervals. Such an under-determined problem has an infinite number of mathematical solutions, many of them without an acceptable physical meaning. As a consequence, to obtain a sensible solution from BBS measurements, it is necessary to restrict the space of solutions by including some a priori information about the neutron spectrum. This information is usually derived by the physical properties of the

neutron field in which the measurements are performed. In general, there are two ways of implementing the a priori information about the measured neutron spectrum for almost all the unfolding codes[7]:

a) By taking an initial guess or default spectrum, with non-negative values Φ_j^{DEF} at each energy bins *Ej* , to start the iteration process.
b) By representing the unknown spectrum with a parameterized function based on physical meaning.

For the former case, the initial guess spectrum can be obtained from Monte Carlo simulations or from previous measurements performed in limited energy ranges with complementary neutron spectrometry systems. In the latter case, the number of parameters adopted must not exceed the number of available measurements, n_S, and should be enough to describe correctly the main features of the neutron spectrum.

To date, the problem of the neutron spectrum unfolding from the BSS measurements has been extensively studied, giving rise to a number of techniques, based on least-square methods, Monte Carlo methods, maximum entropy and Bayesian approach procedures as well as on genetic and neural network algorithms.

2

THE NESCOFI@BTF PROJECT

2.1 Introduction

Neutron fields from thermal to tens or hundreds of MeV are typical of nuclear, medical, industrial or research facilities. These neutron fields may be intentionally generated, as in nuclear power plants or fast neutron irradiation facilities, or may be a parasitic effect, as in accelerator-based cancer therapy. A large interest has gradually arisen and currently exists for on-line neutron spectrometry that would allow to estimate field perturbations due to irradiated objects, to evaluate the importance of room-return for different user positions, and to prevent beam alterations due to any change in energy or space characteristics of the primary beam. Moreover, the medical physics community is seeking on-line instruments able to measure proper quantities for in-phantom or in-vivo characterizations where an accurate knowledge of the neutron spectrum over a wide energy range is required.

Of the many neutron spectrometry techniques available to the scientific community, only the Bonner Sphere Spectrometer (BSS) fulfils this requirement[8]. Whilst polyethylene spheres allow detecting neutrons up to 20 MeV, metal loaded spheres are needed when the neutron energy exceeds this value. The system that uses such modified spheres is called *Extended Range Bonner Sphere Spectrometer* (ERBSS), and is normally equipped with three or more spheres embedding lead, copper or tungsten inserts[9],[10].

2.2 NESCOFI@BTF experiment

The Italian National Institute for Nuclear Physics (INFN), the Politecnico di Milano and the Centro de Investigaciones Energéticas, Medioambientales y Tecnológicas (CIEMAT) of Madrid proposed in 2011 the experiment NEutron Spectrometry in COmplex FIelds @ Beam Test Facility (NESCOFI@BTF). This experiment aims at developing innovative neutron sensitive instruments for the spectrometric and dosimetric characterization of neutron fields intentionally produced or present as parasitic effects in particle accelerators employed for industrial, research and medical applications[11]. Neutron fields typical of these applications are characterized by wide energy distributions, from thermal to tens or hundreds MeV, fluence rates from few tens up to 10^5 cm^{-2} s^{-1}, are accompanied by other particles (photons, high-energy hadrons, etc.), and can have pulsed structure.

To date, as mentioned in chapter 1, the multi-sphere spectrometer is the only existing device having the capability to simultaneously determine all energy components over very large energy intervals (Figure 2.1).

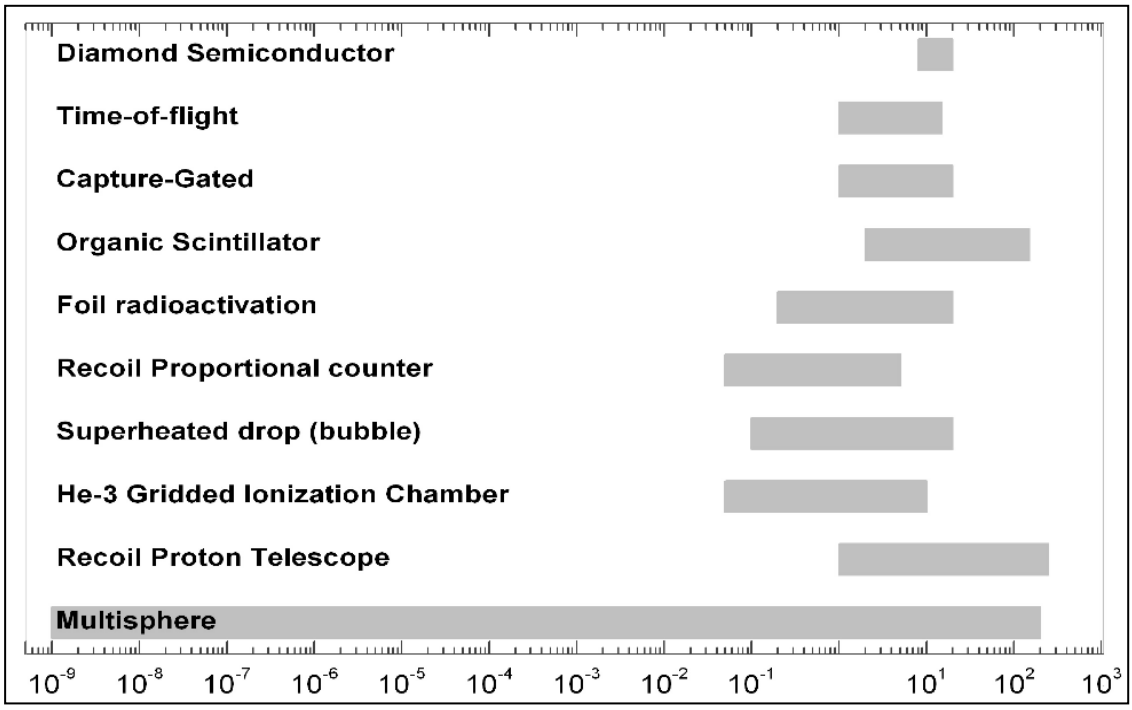

Figure 2.1: Energy range covered by different available neutron spectrometry techniques[12].

The NESCOFI project has the main purpose of realizing real-time spectrometers able to simultaneously provide all energy components in a single irradiation. These feature could be exploited for:

1. monitoring the neutron fields in terms of energy-integrated neutron fluence rate and spectral neutron fluence rate;
2. controlling in real time perturbations induced by changes in the experimental set-up(*e.g.*, targets, samples, materials to be irradiated, patients to be treated, etc.).

The final users of the NESCOFI products will be a variety of facilities interested in monitoring the intensity of a neutron beam and simultaneously its energy and/or direction distribution, which is fundamental in the fields of chip-irradiation, material science, and in particular in research and cancer therapy facilities.

The basic idea behind the project is to exploit the moderation of neutrons in hydrogenated materials, but with new detection systems and computational methods. In particular, the measurement of neutron energy distribution with a single moderator embedding several "direct reading" thermal neutron detectors at different positions is proposed as an effective alternative to the standard multi-spheres approach. More specifically, the project aims at developing two types of real-time spectrometers for different neutron field geometries:

- a CYlindrical Spectrometer (CYSP), either meant for collimated neutron beams or suitable for determining the neutron spectrum in a well defined direction, thus eliminating all other components;
- two SPherical SPectrometers $(SP)^2$, aimed at measuring the neutron fluence spectrum independently from its direction distribution: the first, called *Low-energy* SP^2, for neutron energies up to 20 MeV, and the other, named *High-energy* SP^2, for neutron energies up to hundreds MeV.

In both cases, the energy or angle distribution of the neutron field will be obtained by using unfolding algorithms relying on both the device response matrix and the readings of the different detectors.

2.3 Passive Spherical Spectrometers

As far as the Spherical Spectrometers concerns, a simulation campaign was carried out to identify the appropriate moderator dimension and internal distribution of the thermal neutron detectors. The resulting design embeds 37 or 31 (according to the version, Low-energy or High-energy respectively) thermal neutron detectors. The detectors are symmetrically positioned along three perpendicular axes.

The Low-energy prototype is a 30 cm polyethylene sphere embedding 37 measurement positions. It has spectrometric capability from thermal neutrons up to 20 MeV.

The High-energy version has 25 cm diameter and includes 31 measurement positions. It includes a 1 cm lead shell having inner diameter 3.5 cm. This acts as (n, xn) degrader and allows extending the energy interval of the response up to hundreds of MeV neutrons.

Both Low-energy and High-energy versions have been fabricated and tested in neutron field with well-known energy distribution, with the aim of experimentally confirming the device response matrix, previously determined with Monte Carlo codes. The prototypes were equipped with well-established passive detectors, consisted in Dysprosium activation foils (Figures 2.2 and 2.3).

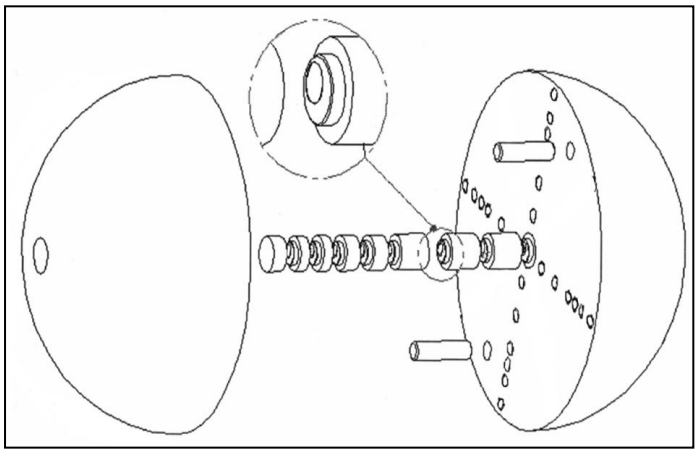

Figure 2.2: Sketch and image of the multidetector Low-energy spectrometer, showing the arrangement of the passive detectors along three perpendicular axes.

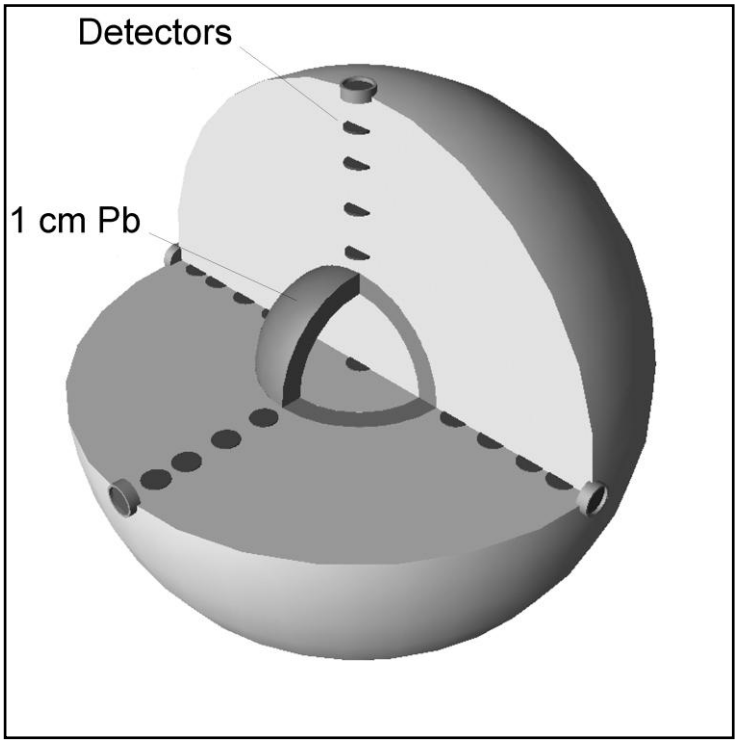

Figure 2.3: Schematic view and image of the internal part of the High-energy spectrometer, showing the arrangement of the activation foils detectors along three perpendicular axes, as well as the inner lead layer.

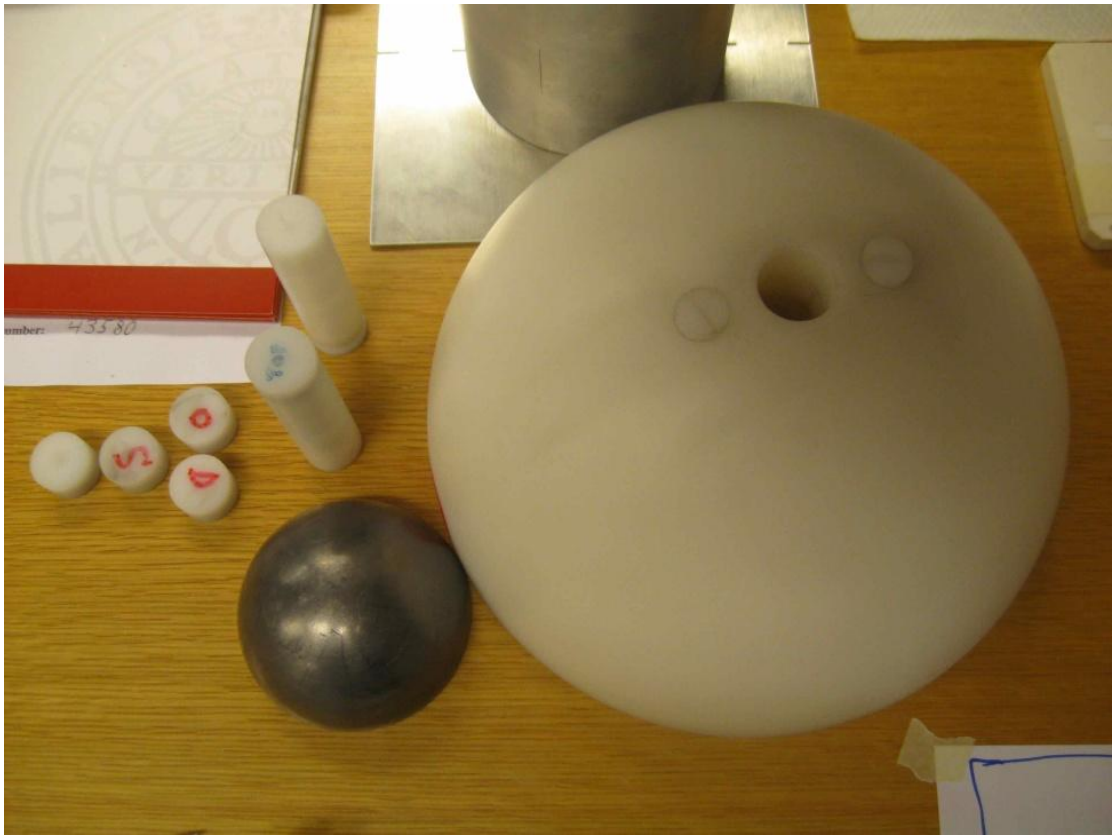

The prototype Low-energy SP^2, equipped with Dy activation foils, was tested in neutron fields previously characterized by a well-known Bonner Sphere spectrometers[13]. The experimental results confirmed that:

- the device has spectrometric capability and similar performance as a standard Bonner Sphere spectrometer, but with the notable advantage of requiring a single exposure.
- The response matrix of the device, determined with Monte Carlo simulation codes, is known with very limited uncertainty (3% in terms of overall error).

The prototype High-energy SP^2, equipped with Dy activation foils, was tested in calibration neutron fields at PTB Braunschweig (monoenergetic fields at 144 keV, 565 keV, 1.2 MeV, 5 MeV, 14.8 MeV) and TSL Uppsala (quasi monoenergetic fields at 50, 100, 150 and 180 MeV plus ANITA, a white spectrum with end point at 180 MeV). The analysis of these data are currently under elaboration, but preliminary results show that the experimental and the calculated responses generally differ by less than 5% for all energies.

Publications Ref. [13, 14] describe the mentioned studies and demonstrate the spectrometric capability of the prototypes.

2.4 Cylindrical Spectrometer

As far as the Cylindrical Spectrometer concerns, a simulation campaign is still in progress to identify the appropriate definitive moderator dimension and internal distribution of the thermal neutron detectors. This type of spectrometer should contain a suitable collimator to eliminate the components from other directions than that of the primary neutron beam and it will also hold a layer of high Z material as an energy shifter for high-energy neutrons.

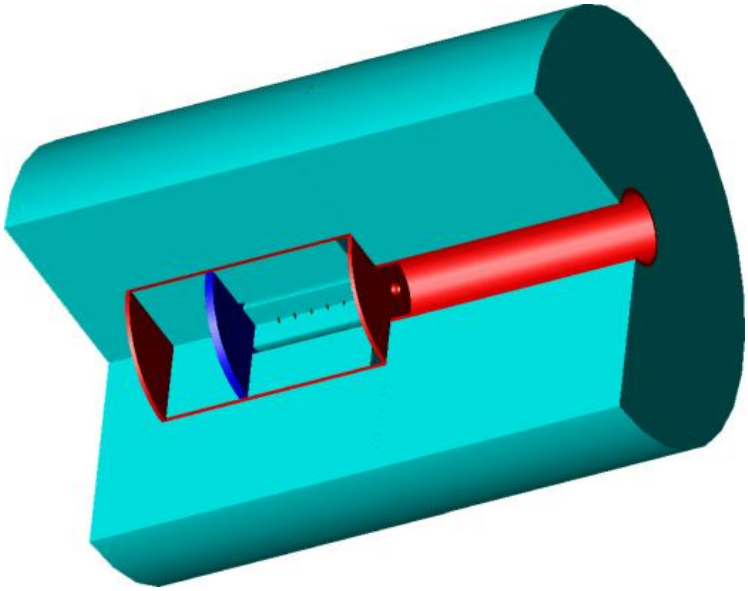

Figure 2.4: Preliminary schematic view of the internal part of the Cylindrical Spectrometer, showing the collimator (red), the energy shifter (blue) and the arrangement of the thermal neutron sensors along its axis.

A low-cost prototype of the Cylindrical Spectrometer, called *Mini-Cysp*, was developed with the aim of performing some irradiation tests. It was not a definitive configuration, but only a simplified 40 cm diameter and 50 cm height cylinder, made of polyethylene, equipped with seven internal cavities equally spaced along its axis.

Irradiation tests of the Mini-Cysp prototype are described in the fourth chapter of this work.

2.5 Conclusions

Active thermal neutron detectors, whose study and development were part of this master Thesis, will replace the passive detectors in the final spectrometers. The resulting instruments will be real-time spectrometers able to simultaneously provide all energy components of the neutron field in a single irradiation.

The selection of the proper active sensor must be based on three fundamental aspects: adequate neutron response (defined as the ratio of the number of counts to the incident thermal neutron fluence), size and cost. The maximum available area of the internal cavities of the final spectrometers is about 1.5×1.5 cm^2 and the unit cost of the neutron sensor has to be not prohibitive, because of the considerable number of detectors to be embedded (37 in the Low-energy SP^2, 31 in the High-energy SP^2 and about 8 in the CYSP).

3

DEVELOPMENT OF ACTIVE THERMAL NEUTRON DETECTORS AND DAQ SYSTEM

3.1 Introduction

The present chapter describes the study and the development of suitable *direct reading* thermal neutron detectors to be used in the spectrometers proposed in the framework of the NESCOFI@BTF Project. Moreover the Data AcQuisition system for the processing and acquisition of signals generated by the Active Thermal Neutron Detectors (ATND) is discussed. As previously mentioned, these sensors must satisfy, at the same time, three main requirements: high neutron response, small size and low cost.

The characterization of suitable active probes is described in the first part of this chapter. Irradiations in thermal neutron field were carried out in order to experimentally determine their performances. It should be underlined that all information concerning the ATND design and fabrication are patent pending.

In the second part the data acquisition system for signals coming from multiple detectors is illustrated. A dedicated Labview2010 program, whose purpose is to simultaneously acquire and process pulses provided by eight different detectors, is explained.

3.2 Active detectors: operation modes

Considering a detector whose response to a single particle or quantum of radiation is a current that flows for a time equal to the charge collection time t_c, the total amount of charge produced in that specific interaction is:

$$Q_{rad} = \frac{E_{rad}}{w} q = \int_0^{t_c} i(t)dt \tag{3.1}$$

where

- E_{rad} is the average energy of the particle or quantum of radiation deposited in the active volume of the detector;
- w is the average amount of energy required to create a charge carrier;
- $q = 1.6 \cdot 10^{-19}$ C.

In the radiation detection, it is possible to distinguish between two general modes of operation, called *pulse mode* and *current mode*. In the first, each individual particle that interacts in the detector is registered, that is the total charge Q_{rad}. In this case it is possible to measure the energy distribution of the incident radiation. When event rates are very high, the current pulses from successive events may overlap in time, and consequently the pulse mode operation is often replaced by the current mode one, where measurements are made by considering the average current generated by the radiation field.

3.3 Active thermal neutron detectors

A first type of ATND, referred as D1 in the following, was studied and characterized with a neutron field generated by a calibration Am-Be source. Seven samples, D1#1-7, which differ in the neutron sensibility, were fabricated and tested.

Monte Carlo simulations based on an analytical model were carried out in order to make a comparison between the theoretical predictions and the experimental results in terms of both thermal neutron interaction probability and the probability of detection of

the nuclear reaction products. Simulation results provided a maximum detection efficiency of about 4.0 %.

3.3.1 Characterization of ATND with thermal neutrons

The development of the D1 sensor was performed at the Nuclear Measurements Laboratory of the Energy Department (Politecnico di Milano) in collaboration with the Italian National Laboratories of Frascati (Istituto Nazionale di Fisica Nucleare, INFN, Frascati, Italy).

The ATND were irradiated with thermal neutrons in order to test the performances of the devices. Irradiations were performed by exploiting the ^{241}Am-Be source (1 Ci) available at the Italian National Laboratories of Frascati. Neutrons emitted by the source were moderated with a polyethylene cylinder 15 cm in diameter and 18 cm in height. A lead screen 6 mm in thickness was placed between the neutron source and the cylinder surface, in order to suppress the gamma contribution of Americium at 59.54 keV. The experimental set-up is shown in Figure 3.1.

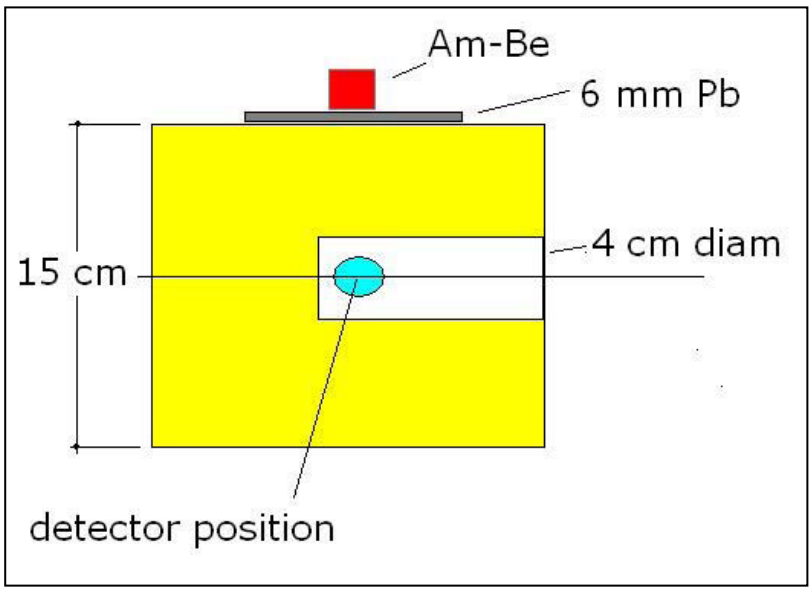

Figure 3.1: Experimental set-up. The ATND was inserted at the center of the cylinder and the neutron source was placed on a lead shield 6 mm in thickness

The ATNDs D1#1-7 were placed, one by one, at the centre of the moderator, at a distance of about 8.1 cm from the neutron source.

Measurements of 3600 s were performed, in pulse mode, for each of the seven ATNDs, in order to select the best in terms of both efficiency and spectrum shape.

The electronic chain consisted in a commercial charge-sensitive preamplifier and in a shaping amplifier module characterized by a gain of 10 and a shaping time equal to 2 μs. This standard chain was included into two different boxes, one for the preamplification stage and the other for the amplification one. The shaped analog linear pulses were then converted into digital pulses by the 2-channel PicoScope 4227 digital oscilloscope, and spectrum processing was performed by means of a dedicated Labview2010 program. The acquisition parameters are listed below:

- measurement time: 3600 s;
- shaping time: 2 μs;
- maximum sample rate: 2 MHz;
- number of spectrum bins: 1024.

3.3.2 Results

The neutron spectrum at the centre of the polyethylene cylinder (Figure 3.2) was simulated through the MCNP code.

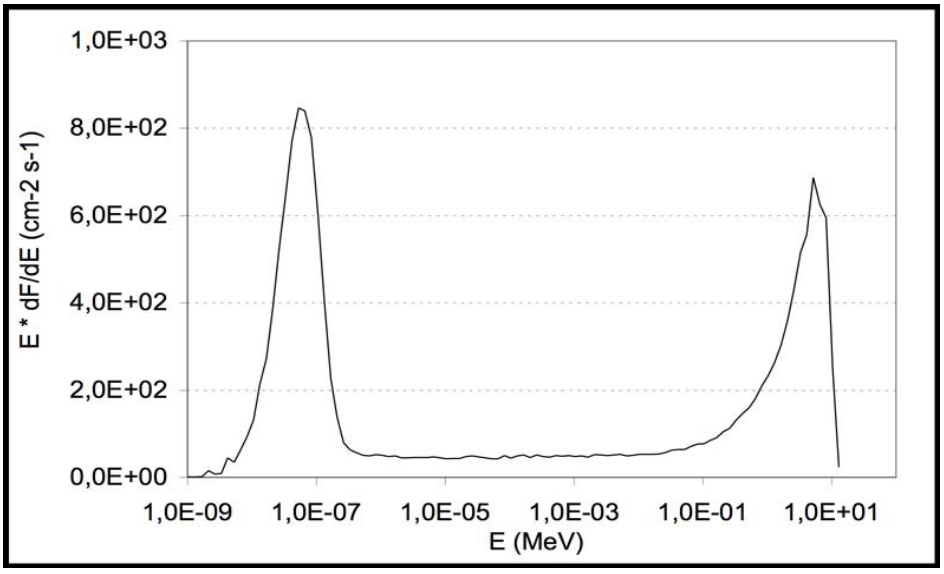

Figure 3.2: Simulated neutron spectrum at the detector position obtained with MCNP.

The thermal (E_n < 0.5 eV) neutron fluence rate at the centre of the cylinder resulted to be equal to $1.49 \cdot 10^3$ cm^{-2} s^{-1}, while the value of the total fluence rate was about $3.30 \cdot 10^3$ cm^{-2} s^{-1}.

Pulse height spectra were obtained and the total counts and counts due to gamma-background were recorded. The net counts, i.e. those due to neutron only, were obtained by subtraction procedure.

Table 3.I: Ratio of total, gamma background and net counts obtained with seven different D1 detectors to that of the #5 probe, taken as a reference.

# of D1detector	Total/#5 [-]	Background/#5 [-]	Net/#5 [-]
1	0.87	1.06	0.61
2	0.97	1.17	0.70
3	1.14	1.37	0.81
4	1.29	1.33	1.23
5	1.00	1.00	1.00
6	0.59	0.65	0.51
7	0.59	0.65	0.50

The ratio of net counts obtained with each probe to that of the #5 probe (taken as a reference) are listed in Table 3.I. As can be observed, sample D1#4 provides the best in detection efficiency. Its thermal neutron response, defined as the ratio of the net count rate to the thermal neutron fluence rate, resulted to be equal to about 0.021 cm^2.

A set of new D1 detectors with the same characteristics of the probe #4 was therefore fabricated.

3.4 Data acquisition system for multiple detectors

The acquisition of signals generated by the detectors was based on a digital technique. In view of the simultaneous acquisition of multiple detectors (more than thirty different ATNDs will be embedded in the final SPherical Spectrometers SP^2), a commercial 8-channel digital oscilloscope (NI USB-6366, National Instruments) was selected. This digitizer provides 8 analog inputs, simultaneously sampled at a maximum rate of 2 MS s^{-1} with a resolution of 16 bits.

Digital filtering and spectrum processing were performed in streaming mode by means of an *ad hoc* developed Labview2010 program, called "8-channels acquisition.vi". This program, entirely developed in the framework of this master Thesis, provides four different panels, called *Set-up*, *Signals*, *Spectra* and *Count Rate* (Figures 3.3a, 3.3b, 3.3c and 3.3d).

a) Set-up: in this panel, it is possible to set up:

- the *Trigger level*, defined as the threshold (in Volts) from which to start acquiring samples, specifying both which *Slope* (falling or rising) to trigger on, and the name of a virtual channel where there is an analog signal to be employed as the *Source* of the trigger;
- the names of the *Physical channels* to use to create virtual channels, from a minimum of one to a maximum of eight channels. The DAQmx physical channel constant lists all the physical channels on devices and modules installed in the system. A box on top of the screen shows the number and the name of the active channels;
- *Maximum* and *Minimum* values (in Volts) expected to be measured;
- *Sampling rate* (in sample per channel per second);
- *Buffer size* (in sample per channel), defined as the number of samples the buffer can hold for each channel in the task.

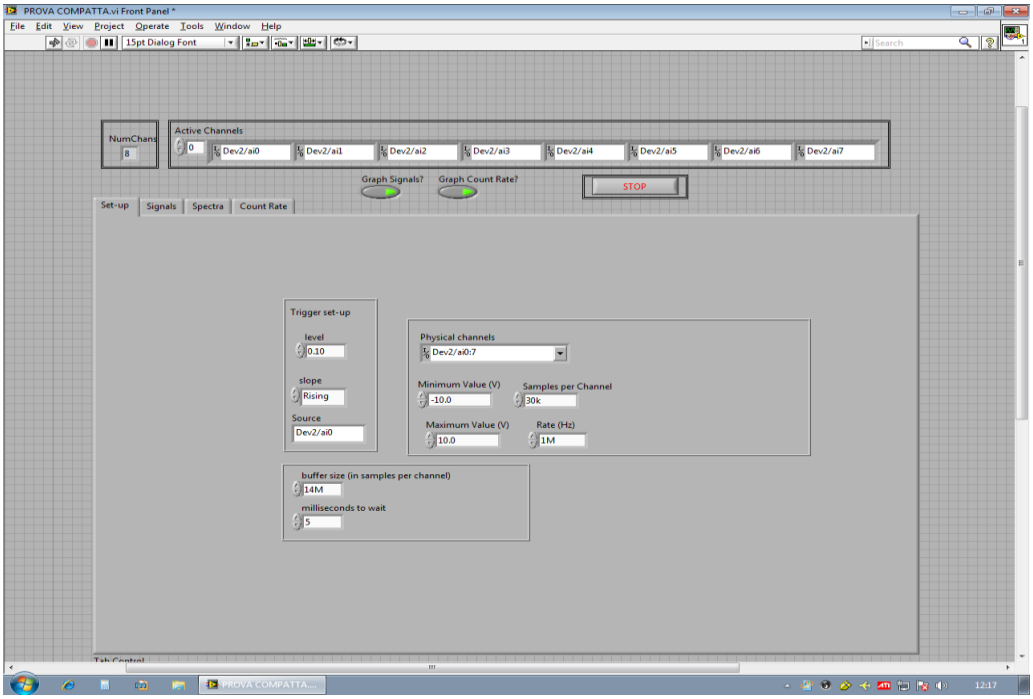

Figure 3.3a: Panel *Set Up* of the "8-channels acquisition.vi" Labview 2010 program.

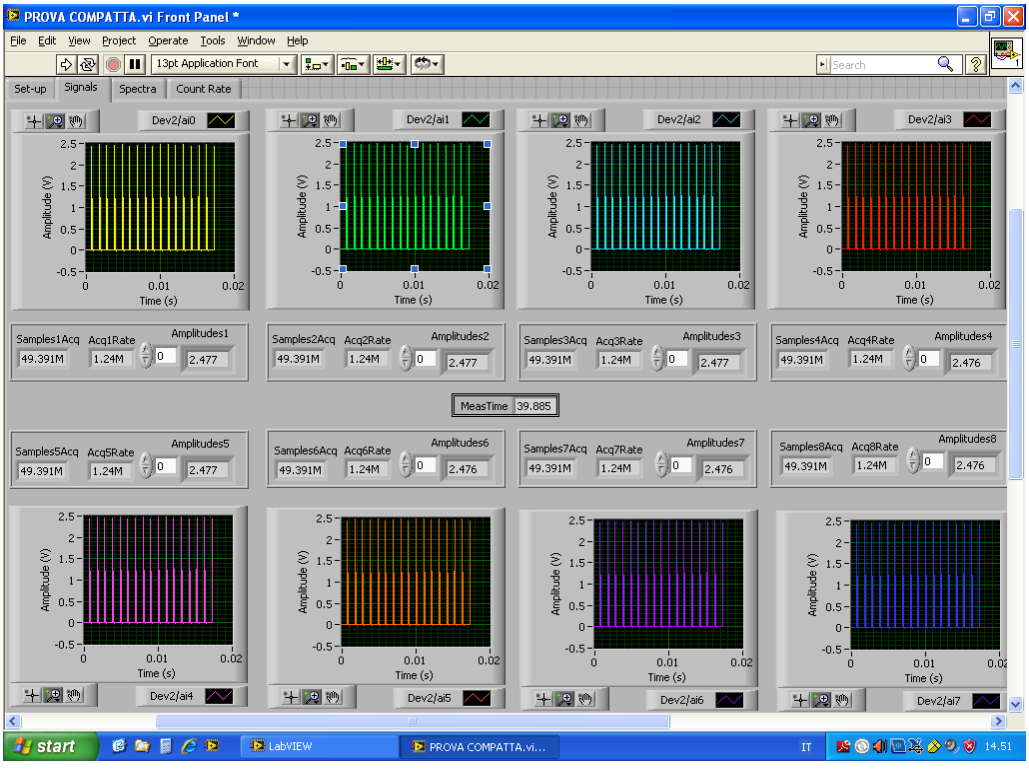

Figure 3.3b: Panel *Signals* of the "8-channels acquisition.vi" Labview 2010 program.

b) Signals: this box displays a signal graph and three indicators for each of the active channels real-time. The number of *Acquired samples*, the actual *Acquisition rate* and the *Measurement time* are indicated.

At this point of the program, a *Waveform peak detector* function is employed in order to find the *Locations* and the *Amplitudes* of the peaks in the input signal. This function is based on an algorithm that fits a quadratic polynomial to sequential groups of data points. The parameter *Width*, which is located in the next panel, specifies the number of these consecutive data points to use in the quadratic least squares fit. This value should be not higher than about ½ of the peak half-width, and no less than 3. In fact, large widths may reduce the apparent amplitude of the peaks and shift their apparent location. Ideally, the width should be as small as possible, but a compromise solution must be opted for so as to prevent the possibility of false peak detection due to electronic noise.

For each peak, the quadratic fit is tested against a threshold, which is set to the same value of the trigger level: peaks with heights lower than this threshold are ignored.

c) Spectra: this panel shows the discrete histogram of the peak amplitudes of the input signal for each of the active channels real time. The *y*-axis represents the histogram count, and the *x*-axis represents the histogram center values of the intervals or bins, in Volts. Four parameters must be set:

- the *Maximum* and *Minimum* values (in Volts) to be included in the histogram;
- the *Number of bins* in the histogram;
- the number of consecutive data points (*Width*) to use in the quadratic least squares fit.

The value of the integral *Counts* between the maximum and minimum values of the spectrum is indicated.

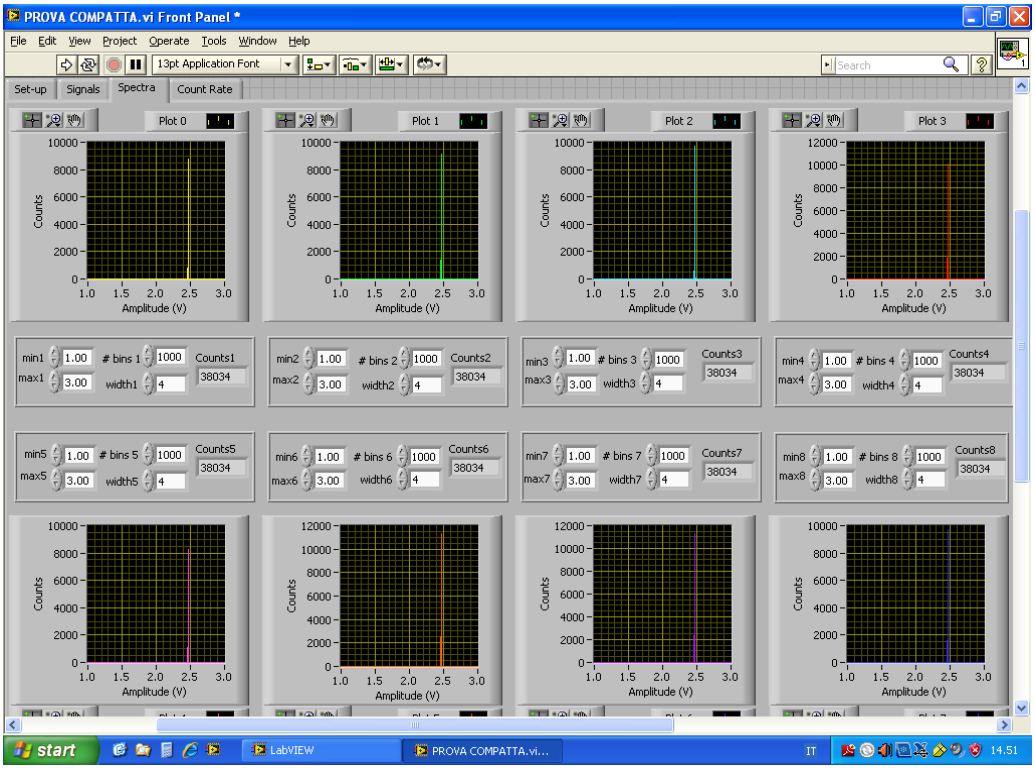

Figure 3.3c: Panel *Spectra* of the "8-channels acquisition.vi" Labview 2010 program.

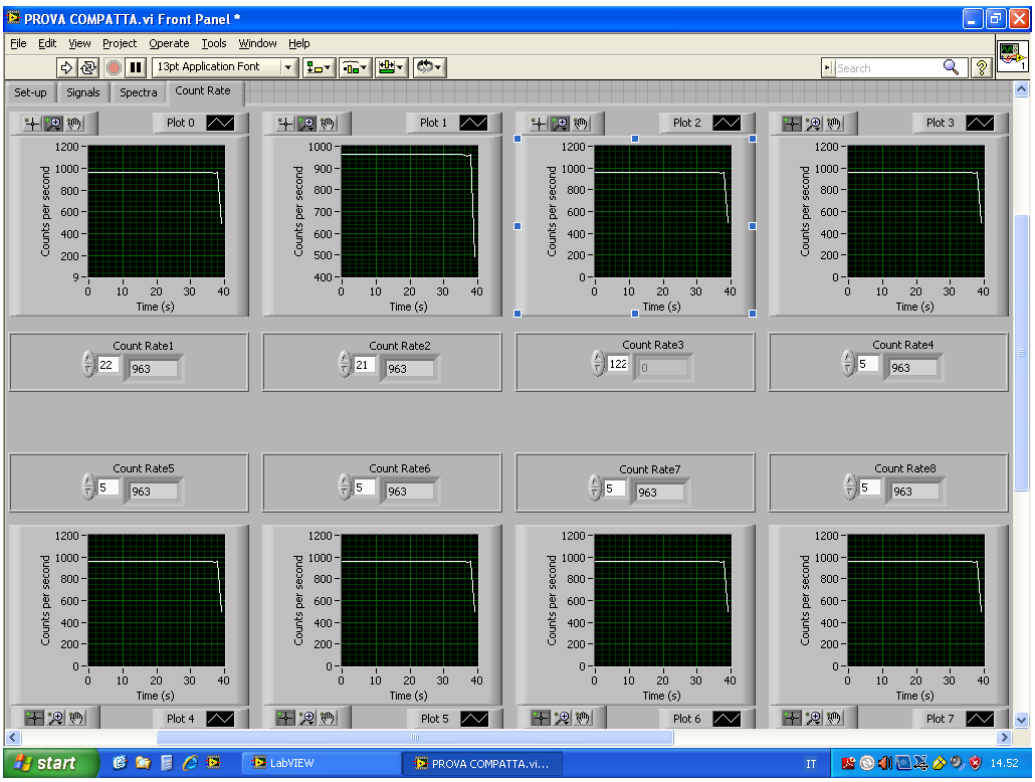

Figure 3.3d: Panel *Count Rate* of the "8-channels acquisition.vi" Labview 2010 program.

d) Count Rate: this final screen displays the trend of the count rate (in counts per second) as a function of time.

At the end of each measurement, the spectra related to the active channels are recorded, along with the acquisition parameters set in the first three panels.

The data acquisition section of the "8-channels acquisition.vi" Labview2010 program exploits some functions given by the NI-DAQmx software of the National Instruments.

At the very beginning of the program, a *DAQmx Create Virtual Channel* function was utilized, with the aim of creating virtual channels to measure A/I voltage and adding them to a *task*, defined as a collection of one or more virtual channels with timing, triggering, and other properties. Virtual channels are software entities that encapsulate the physical channel along with other channel specific information (range, terminal configuration, and user scaling) that formats the data. The *DAQmx physical channel* constant lists all physical channels on devices and modules installed in the system. A physical channel is a terminal or pin at which you can measure an analog signal and it can include more than one terminal, as in the case of a differential analog input. Every physical channel on a device has a unique name.
Maximum and minimum values specifies the maximum and minimum value, in Volts, you expect to measure.

Then the *DAQmx Timing* function allows to select the onboard clock of the device as the source of the sample clock and to set the sampling rate (in samples per channel per second). It is possible to acquire a finite number of samples or to acquire samples continuously until the *DAQmx Stop Task* VI runs.

Subsequently the *DAQmx Trigger* function was exploited in order to configures the task to start acquiring samples when an analog signal crosses a set Trigger level on a rising slope.

Finally a *DAQmx Read* function was used to read one or more waveforms from the task previously created. If the task acquires samples continuously, this VI reads all the samples currently available in the buffer. This function returns a 1D array of waveforms

and each element of the array corresponds to a channel in the task. The order of the channels in the array corresponds to the order in which the user adds the channels to the task.

After the 1D array of waveforms has been acquired, the data elaboration section of the "8-channels acquisition.vi" program, which includes two main different dedicated *subVIs*, is launched. These stages, initially developed and improved in order to elaborate signals from only one physical channel, were then parallelized with the aim of simultaneously processing data from eight different channels.

- The *first subVI* selects the *i*-channel from the 1D array of waveforms, where the index *i* ranges from 0 (first channel) to 7 (eighth channel) and makes the relative signal graph. A *Waveform Peak Detection VI* finds the locations and amplitudes of peaks (above a set threshold value) in the waveform, via a quadratic least square fit.

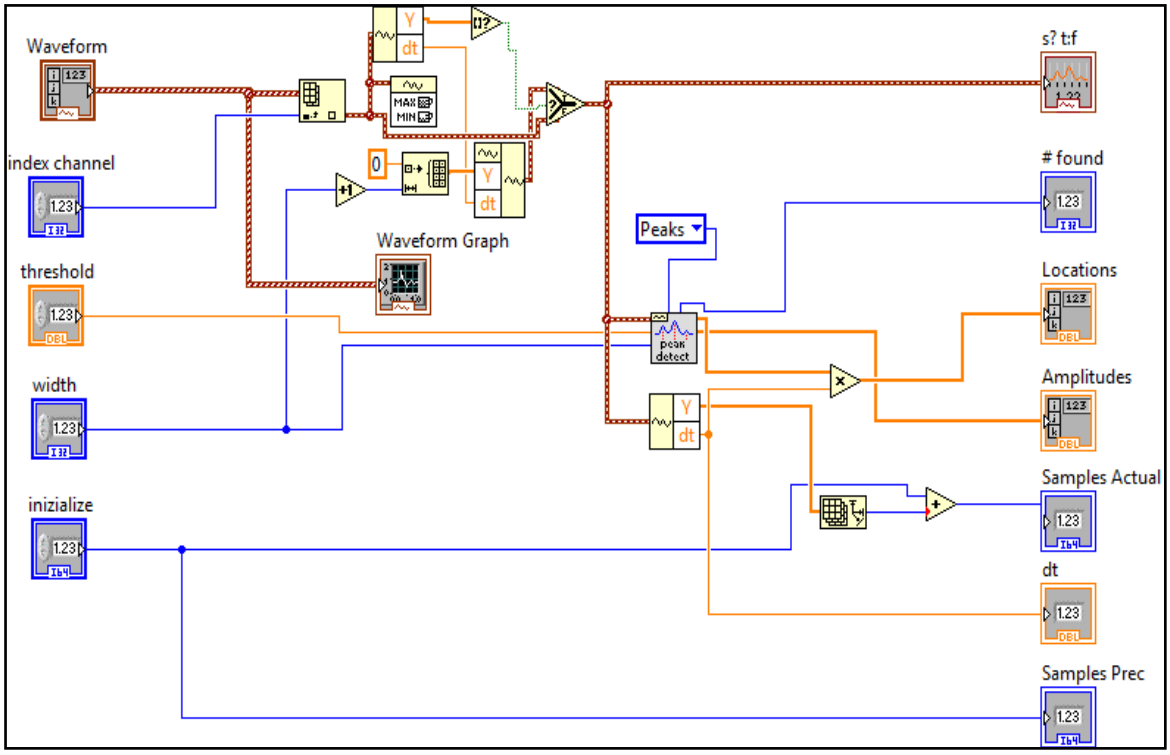

Figure 3.4: Structure of the first *SubVI* of the **"**8-channels acquisition.vi" Labview 2010 program.

- The *second subVI* receives the amplitudes of peaks as input and finds the discrete histogram, based on three bin specifications given by the user: the maximum and minimum values *M* and *m* to include in the histogram and the number of bins *k*.
  The *General Histogram VI* completes the following steps to obtain the final histogram: it establishes all the bins, defines the function $y_i(x)$ and evaluates the histogram sequence H. Each bin width Δx is the same and it is defined with the following relation:

$$\Delta x = \frac{M-m}{k} \tag{3.2}$$

A *lower inclusion* was selected, in order to include the lower boundary of each bin. The bin widths are determined according to the following equations:

$$\begin{aligned} \Delta_0 &= [m : m + \Delta x) \\ \Delta_1 &= [m + \Delta x : m + 2\Delta x) \\ \Delta_i &= [m + i\Delta x : m + (i+1)\Delta x) \\ \Delta_{k-1} &= [m + (k-1)\Delta x : M] \end{aligned} \tag{3.3}$$

It is important to note that the first start point *m* and last end point *M* are always included in the first and last bins.
The function $y_i(x)$ is given by the following relation:

$$y_i(x) = \begin{cases} 1 & if\ x\ is\ included\ in\ \Delta_i \\ 0 & elsewhere \end{cases} \tag{3.4}$$

The *General Hisotgram VI* then evaluates the histogram sequence with the following equation:

$$h_i = \sum_{j=0}^{n-1} y_i(x_j) \tag{3.5}$$

where *n* is the number of elements in the input sequence of amplitudes and h_i is the total number of points in the input array that fall into the bin Δ_i.

Finally the bar graph of the histogram of the input sequence is displayed. The y-axis is the histogram count, and the x-axis is the histogram center values of the intervals (bins) of the histogram.

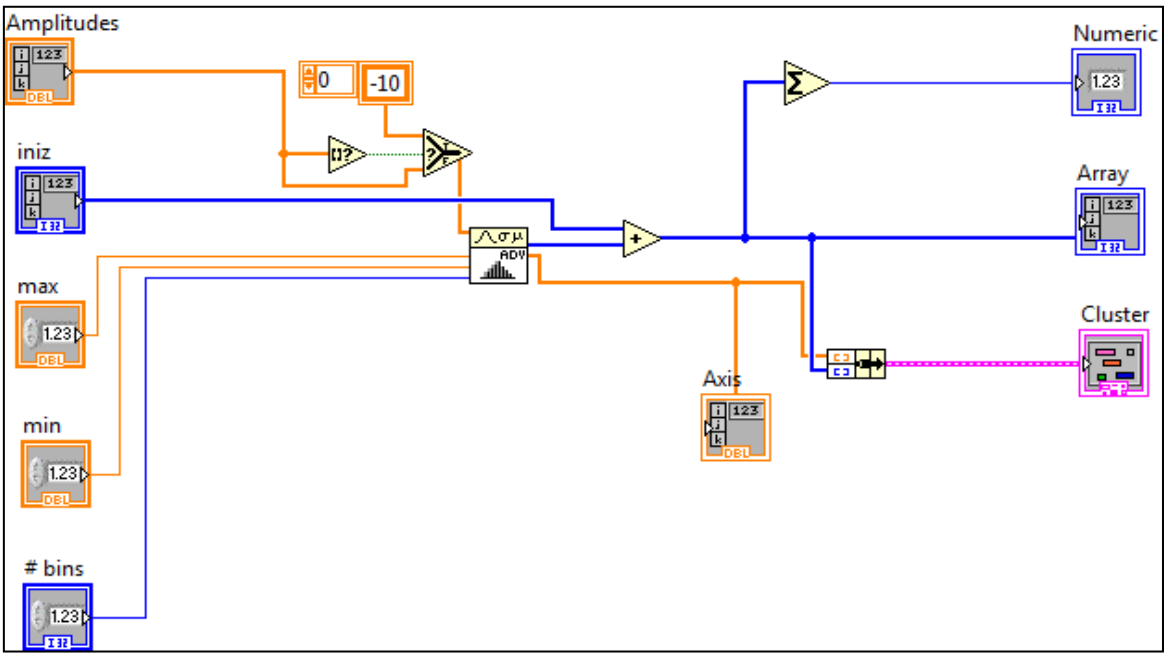

Figure 3.5: Structure of the second *SubVI* of the **"**8-channels acquisition.vi" Labview 2010 program.

As far as the performance of the NI USB-6366 digital oscilloscope is concerned, even though a sample rate equal to 2 MS s^{-1} for each channel is declared, some tests performed with different numbers of active channels (from one to eight) show that the "8-channels acquisition.vi" program works properly at 2 MS s^{-1} only with up to five active channels. When turning all eight channels on, the maximum sample rate is equal to 1.25 MS s^{-1} per channel.

The best found solution is to disable the visualization of the graphics of the signals and/or that of the count rates, thanks to two *Case Structures* and two Boolean values which can be set by the user, called *Graph signals?* and *Graph Count Rate?*, respectively.

4

APPLICATION OF ATND IN THE MINI-CYLINDRICAL SPECTROMETER

4.1 Introduction

The basic idea behind the NESCOFI@BTF project is to exploit the moderation of neutrons in hydrogenated materials by employing a single moderator embedding several "direct reading" thermal neutron detectors at different positions.

A low-cost prototype of the Cylindrical Spectrometer, called *Mini-Cysp*, was developed with the aim of performing some irradiation tests. The cylindrical prototype was equipped with the D1#4 active sensors, described in chapter 3.

The Mini-Cysp was not a definitive configuration, but only a simplified 40 cm diameter and 50 cm height cylinder, made of polyethylene, provided with seven internal cavities equally spaced along its axis into which the active sensors were placed.

4.2 Experimental set-up

Irradiation tests of the Mini-Cysp prototype were performed in the free-scattering facility of the National Physical Laboratory in London. Irradiations were performed with 5 MeV and 565 keV neutrons produced by protons or deuterons accelerated by the 3.5 MV Van de Graaff accelerator. In particular, neutrons were produced at 5 MeV using the D(d, n)^{3}He reaction and at 565 keV using the ^{7}Li(p, n)^{7}Be reaction.

The Mini-Cysp was placed at 150.5 cm from the target, at 0°, with the central axis along the beam line.

Figure 4.1: Experimental set-up. The distance from the neutron producing target to the end of the cylinder was equal to 150.5 cm.

In order to characterize the neutron response of the D1 ATND, two measurements were performed, with and without shadow-cone (Figure 4.2).

Figure 4.2: Experimental set-up for measurements of the total neutron field (left) and of the only scatter component by using a shadow cone (right).

Analog signals from seven sensors were processed by using 4 indipendent electronic chains assembled ad hoc for the Mini-Cysp characterization. Figure 4.3 shows a picture of these chains, constituted by commercial charge-sensitive preamplifiers and a shaping amplifier modules assembled into eight different boxes, four for the preamps and four for the amplifiers.

The shaped analog linear pulses were then converted into digital pulses by using the 8-channel NI USB-6366 digital oscilloscope. Simultaneous data acquisition and elaboration were performed by using the "8-channels acquisition.vi" Labview 2010 program described in chapter 3.

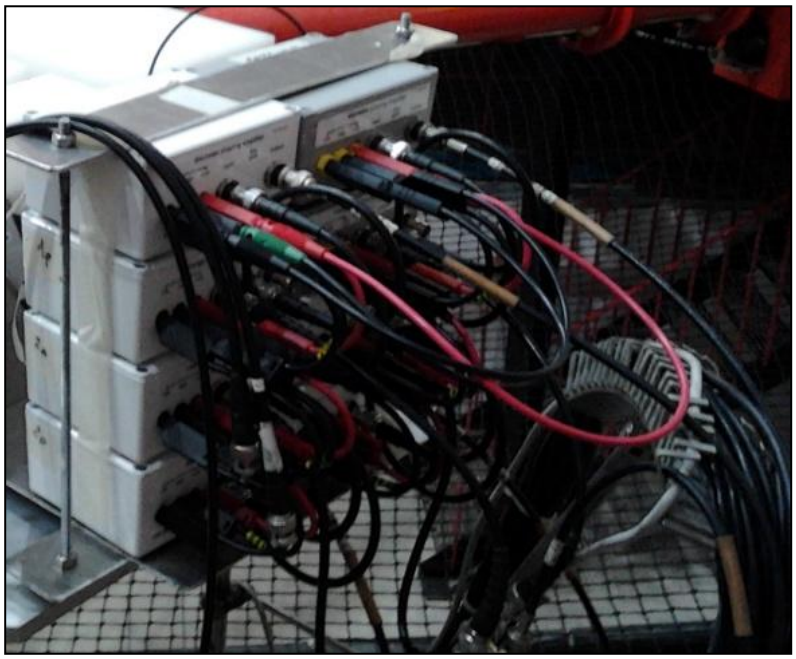

Figure 4.3: Electronic chains for 4 different detectors (2 boxes for each chain).

4.3 Results

Neutron fluence estimated at the entrance of the cylinder resulted to be about $1.03 \cdot 10^6 cm^{-2}$ and $3.27 \cdot 10^6$ cm^{-2}, for 5 MeV and 565 keV neutrons, respectively.

Figure 4.4 illustrates the seven measurement positions of the ATND inside the Mini-Cysp. Experimental results are reported in table 4.I.

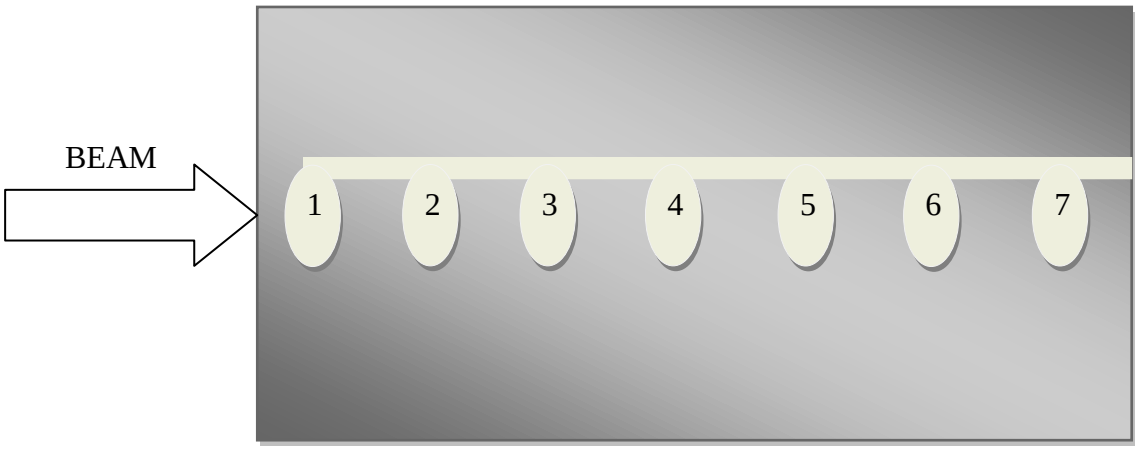

Figure 4.4: Section of the Mini-Cysp. Seven internal cavities equally spaced along the cylinder axis contain seven D1 active thermal neutron detectors. A groove from the first position to the end of the cylinder accommodates as many connecting cables.

Table 4.I: Counts and counts per unit neutron fluence of the seven detectors embedded in the Miny-Cysp, obtained with 5 MeV and 565 keV neutron irradiations.

	5 MeV		**565 keV**	
Position	**Counts [-]**	**Counts/fluence [10^{-3} cm^2]**	**Counts [-]**	**Counts/fluence [10^{-3} cm^2]**
1	6673 ± 82	6.5 ± 0.4	16880 ± 130	16.4 ± 0.9
2	10203 ± 101	9.9 ± 0.5	12971 ± 114	12.6 ± 0.7
3	8430 ± 92	8.2 ± 0.4	3944 ± 63	3.8 ± 0.2
4	4428 ± 67	4.3 ± 0.2	2268 ± 48	2.2 ± 0.1
5	1962 ± 44	1.9 ± 0.1	1447 ± 38	1.4 ± 0.08
6	732 ± 27	0.7 ± 0.05	1118 ± 33	1.1 ± 0.07
7	608 ± 25	0.6 ± 0.04	1019 ± 32	1.0 ± 0.06

The trend of counts per unit neutron fluence as a function of the detector position is shown in Figure 4.5, for both 5 MeV and 565 keV irradiations.

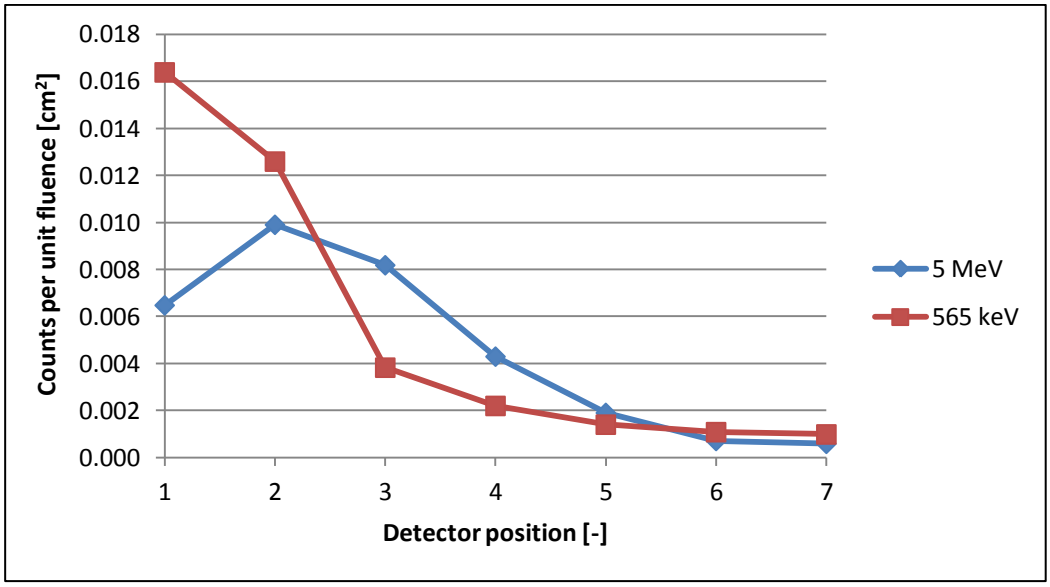

Figure 4.5: Counts per unit fluence as a function of the detector position, for both 5 MeV and 565 keV irradiations.

Results obtained by using a shadow cone show that the scattered component of the neutron field is negligible for almost all the detector positions, except for the first one: in this case, the contribution of the scattered component was about 8% for 5 MeV neutron and 2% for 565 keV.

4.4 Conclusions and comments

The preliminary irradiations performed at NPL confirmed the possibility of simultaneously acquire and elaborate signals from different active thermal neutron detectors within a single moderating structure. The final CYlindrical SPectrometer will contain a suitable collimator to eliminate the scattered components. It will hold also a layer of high Z material as an energy shifter for high-energy neutrons.

Nevertheless, some criticalities were highlighted by these test measurements, in particular about the analysis of the D1 sensor response (a) and about the commercial electronics adopted (b).

As far as the point (a) concerns, two different aspects must be considered:

- The discrimination between gamma and neutron signals in the pulse height spectra resulted particularly complex, since gamma and neutron signals were overlapped in some areas of the spectrum. Since a large number of counts was necessarily neglected to ensure the selection of the pure neutron contribution, the final efficiency resulted significantly lower than the expected one.
- The amplitude of the signals due to thermal neutrons was very close to the acquisition threshold value. Even a small increase in the electronic noise associated with the acquisition system or the presence of a interference source necessary affects the measurement.

Regarding the point (b), the single electronic chain (for the single detector) was the same chain utilized in the previous characterization of the D1 ATND in thermal neutron fields. It consisted in a commercial charge-sensitive preamplifier and in a shaping amplifier module characterized by a gain of 10 and a shaping time equal to 2 μs, and it was included into two different boxes, one for the preamplification stage and the other for the amplification one.

This did not constitute a problem in terms of space when working with only one or two detectors, but it was an issue in the case of many detectors. Moreover, the management of many discrete electronic components, as especially regards the localization of any extrinsic noise sources (for instance the ground loops arising from currents flowing in the ground path of the circuit) and their removal, resulted quite difficult.

5

MULTI-CHANNEL ELECTRONICS AND NEW ACTIVE DETECTORS

5.1 Electronic integrated boards

The irradiation tests of the Mini-Cysp prototype embedding several D1 active detectors pointed out some criticalities to face, regarding both the discrete acquisition electronics and the neutron response of the active sensors.

As mentioned before, the exploitation of multiple discrete electronic chains, each of which consisted in a commercial charge-sensitive preamplifier and in a shaping amplifier module, appeared rather difficult. For this reason, in view of the simultaneous acquisition of multiple detectors, these stages were integrated and parallelized in portable 2-channel and 8-channel boards.

Figure 5.1 shows a picture of the 8-channel board. The 2-channel board, inserted in a metal box, is shown in Figure 5.2.

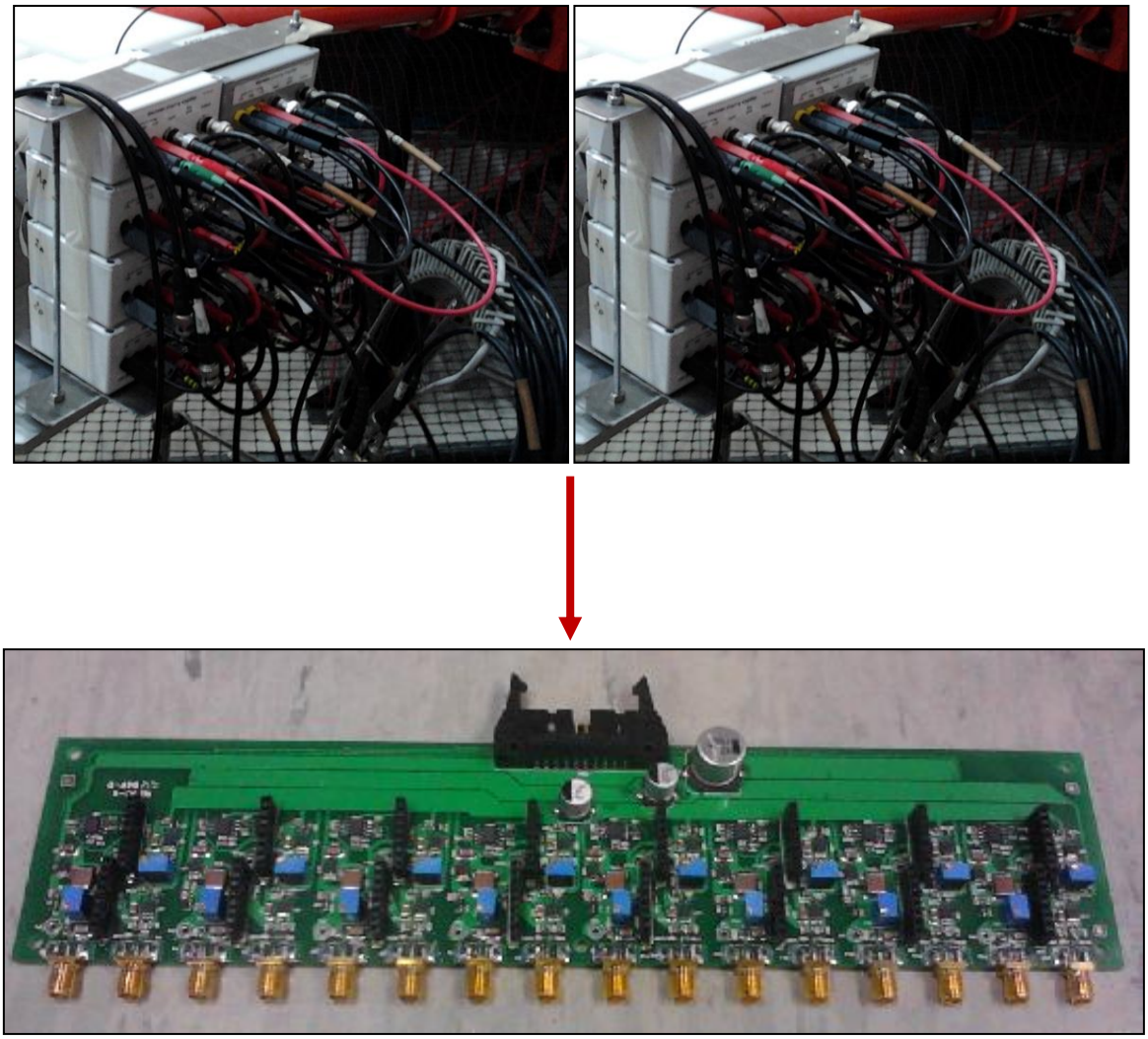

Figure 5.1: Electronic chains (up) for 8 different detectors (2 boxes for each chain). These discrete components were replaced with an 8-channel integrated board (down).

All channels are independent, and each of them consists in:

- a detector input;
- a test input;
- a commercial charge-sensitive preamplifier module;
- a commercial linear shaping amplifier;
- independent power supplies;
- an output buffer which drives 50 Ω coaxial cables.

Figure 5.2: The 2-channel board was inserted in a metal box, in order to shield the circuit from the environmental electromagnetic noise.

5.2 New active thermal neutron detectors

The second critical aspect highlighted during the NPL irradiation tests concerns the thermal neutron response of the D1 sensor. The discrimination between gamma and neutron counts in the pulse height spectra was not effective, owing to the overlapping of the two contributions. Furthermore, the amplitude of signals due to thermal neutrons was very close to the acquisition threshold value.

In order to overcome these two practical problems, it was decided to develop another type of active thermal neutron detector, by taking into account the same requirements about neutron response, size and cost.

All data about the type of detector and the phases of its development will be omitted being patent pending.

A new preliminary study about another ATND, called D2 in the following, was performed. Six samples, D2#1-6, which differ in the neutron sensibility, were developed.

Monte Carlo simulations based on an analytical model were carried out in order to make a comparison between the theoretical predictions and the experimental results in

terms of both thermal neutron interaction probability and the probability of detection of the nuclear reaction products. Simulation results provided a maximum detection efficiency of about 4.8 %.

5.2.1 Characterization of D2 ATND with thermal neutrons

The development of the D2 sensor was performed at the Nuclear Measurements Laboratory of the Energy Department (Politecnico di Milano) in collaboration with the Italian National Laboratories of Frascati. The D2#1-6 ATND were irradiated with thermal neutrons generated by an Am-Be source in order to test the their performances. The same experimental set-up used for the characterization of the D1 sensors was exploited in order to evaluate and compare the performances of D1 and D2 type.

Measurements of 3600 s were performed for each of the six ATNDs, in order to select the best in terms of both efficiency and spectrum features. The portable 2-channel board previously described was used. The shaped analog linear pulses were then converted into digital pulses by the 2-channel PicoScope 4227 digital oscilloscope, and signal processing was performed by means of a dedicated Labview2010 program. The acquisition parameters are listed below:

- measurement time: 3600 s;
- shaping time: 2 μs;
- maximum sample rate: 2 MHz;
- number of spectrum bins: 1024.

5.2.2 Results

Six spectra were acquired. Compared with the results obtained when using the D1 detector, these spectra are shifted towards higher signal amplitudes, thus making the *n*-γ discrimination easier. Counts from a proper threshold value to the end of the scale are due exclusively to the thermal neutron field.

Considering the integral counts from a proper threshold, the response of the different detectors, defined as the ratio of the count rate to the thermal neutron fluence

rate simulated by MCNP, are listed in Table 5.I. On the basis of these data, the more sensitive probe results the D2#6 .

Table 5.I: Net counts, due to thermal neutron contribution, and responses of the six D2 detectors.

# of D2 detector	Net counts [-]	Net counts / #6 counts [-]	Response [cm^2]
1	18921	0.14	0.004
2	38171	0.28	0.007
3	67487	0.50	0.013
4	81391	0.60	0.015
5	85800	0.63	0.016
6	135104	1.00	0.026

5.3 Comparison between D1 and D2 active thermal neutron detectors

A comparison between the D1#4 and D2#6 detectors was performed. The following major outcomes were achieved:

- the response of the two detectors is similar; in particular, the D2#6 exhibits slightly better performance, being its response equal 0.026 cm^2 *vs.* 0.021 cm^2 for the D1#4;
- the use of the D2 detectors largely enhance the effectiveness of the n-γ discrimination. The spectra obtained by means of the D2 show a net separation between gamma and neutron contribution. A proper threshold is sufficient to derive counts due to neutrons;
- the D1 sensor main advantage of featuring a higher thermal neutron sensibility is balanced (and penalized) by a large photon contribution and a worse signal-to-noise ratio.

For this, the D2 ATND was selected as the best option.

6

APPLICATION OF ATND IN STANDARD BONNER SPHERE SPECTROMETER

6.1 Preliminary measurements with the ERBSS system using the ATND

The ATND D1#4 and D2#6 described in the previous chapters were tested within a standard Extended Range Bonner Sphere Spectrometer System (ERBSS), in order to check their performances in neutron spectrometry. These tests were performed at the PAULA proton beam facility of The Svedberg Laboratory of the Uppsala University (Sweden). The neutron field was generated by 30 MeV protons on a beryllium target.

At present, reference data associated to irradiation, in particular proton beam currents and neutron fluences, are not available yet. Therefore, experimental results refer to the nominal proton current, set at about 50 nA and 200 nA.

Eight standard spheres and one extended range sphere (with a lead shell), (external diameter of about 2, 2.5, 3, 4, 5, 7, 8, 10,12 inches) were exposed to different neutron fields.

Three different ATND placed at the centre of each sphere were used:

- A standard cylindrical lithium iodide scintillator (^{6}LiI (Eu), 4 mm x 4 mm), which was used as the reference;
- A D1#4 active thermal neutron detector.
- A D2#6 active thermal neutron detector.

The purpose of these measurements was to verify that the ratio of ^{6}LiI counts to D1#4 counts and the ratio of ^{6}LiI counts to D2#6 counts are independent on the diameter of the sphere.
The acquisition parameters for the D1 and D2 detectors were:

- Measurement Time: 300 s;
- Shaping time: 2 μs;
- Sample Rate: 2 MHz;
- Number of spectrum bins: 1024.

The experimental set-up is shown in Figure 6.1. All measurements were performed placing the spheres at 2.5 m from the neutron producing target. The different ATND were placed sequentially at the centre of each sphere.

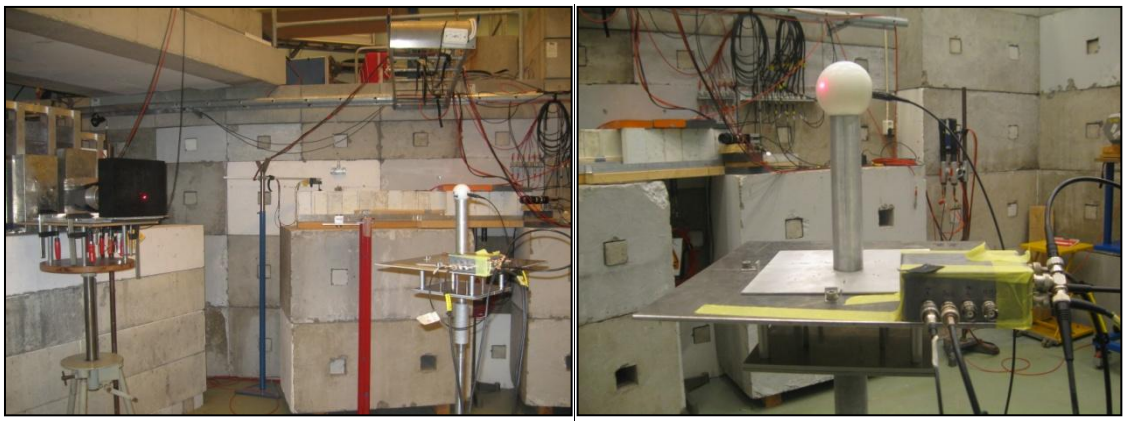

Figure 6.1: Experimental set-up: the point of measurement was at 2.5 m from the neutron producing target.

6.2 Results and conclusions

Figure 6.2 shows the experimental results obtained with the LiI scintillator (blue line), the D1 detector (red line) and the D2 detector (green line), respectively. The nominal value of the cyclotron proton current was equal to 50 nA for the measurements carried out with the LiI scintillator and to 200 nA for the other two systems.

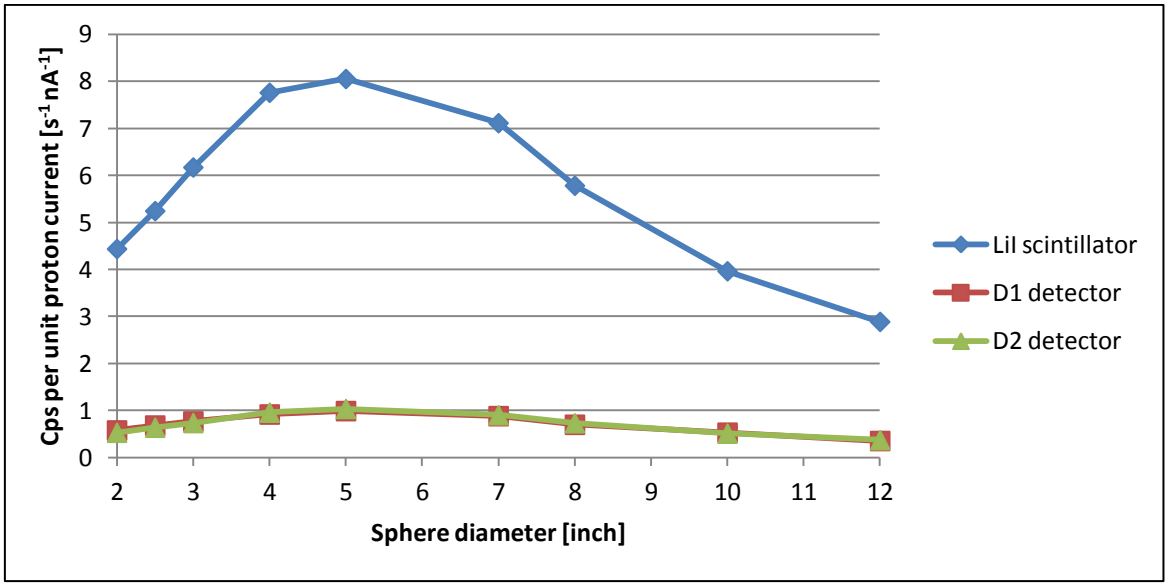

Figure 6.2: Trend of cps per unit proton current due to thermal neutron signal as a function of the BSS sphere diameter.

The ratio of ^{6}LiI cps per unit proton current to D1 ones and that of ^{6}LiI cps per unit proton current to D2 ones are listed in Table 6.I.

Table 6.I: Cps per unit proton current, due to thermal neutron signals, obtained with the LiI scintillator, the D1 detector, and the D2 detector, respectively. The ratio of LiI cps/I_p to D1 and D2 cps/I_p are also indicated. Uncertainties were calculated by assuming a uncertainty equal to 5% in the nominal value of the proton current.

Diameter sphere (inch)	LiI cps/I_p [s^{-1} nA^{-1}]	D1 cps/I_p [s^{-1} nA^{-1}]	D2 cps/I_p [s^{-1} nA^{-1}]	LiI / D1 [-]	LiI / D2 [-]
2	4.44	0.58	0.53	7.66 ± 0.55	8.36 ± 0.59
2.5	5.24	0.68	0.64	7.67 ± 0.55	8.21 ± 0.58
3	6.17	0.77	0.74	8.02 ± 0.57	8.37 ± 0.59
4	7.76	0.92	0.96	8.44 ± 0.60	8.10 ± 0.57
5	8.05	0.99	1.04	8.12 ± 0.58	7.77 ± 0.55
7	7.11	0.88	0.90	8.05 ± 0.57	7.87 ± 0.56
8	5.78	0.70	0.73	8.26 ± 0.59	7.90 ± 0.56
10	3.96	0.53	0.51	7.46 ± 0.53	7.74 ± 0.55
12+Pb	2.89	0.35	0.37	8.14 ± 0.58	7.75 ± 0.55

The average values of the LiI / D1 and the LiI / D2 data are equal to 7.98 and 8.01, showing a relative standard deviation, defined as the ratio of the standard deviation to the average, of 4.0% and 3.2%, respectively.

It should be underlined that these results are only preliminary. A detailed comparison and characterization will be performed when actual reference data for each measurement will be available. In any case, these preliminary comparison demonstrate the agreement between results derive through the D1 and D2 sensor with respect to the reference ^{6}LiI ATND.

In conclusion, the efficiency of the D1 and D2 sensors is about eight times lower than that of the LiI sensor. On the other hand, the great advantage of these new ATND, compared with the scintillator detector, is their very small dimensions and their cheapness.

CONCLUSIONS

The study and the development of suitable active sensors to be used in the spectrometers proposed in the framework of the NESCOFI@BTF Project were carried out. The selection of the proper active detector was based on three fundamental aspects: adequate neutron response, size and cost. The maximum available area of the internal cavities of the final spectrometers is about 1.5×1.5 cm^2 and the unit cost of the neutron sensor has to be not prohibitive, because of the considerable number of detectors to be embedded (37 in the Low-energy SP^2, 31 in the High-energy SP^2 and about 8 in the CYSP).

A first type of ATND, named D1, was studied and characterized with a neutron field generated by a calibration Am-Be source. Seven samples, D1#1-7, which differed in the neutron sensibility, were fabricated and tested. Irradiations with thermal neutrons highlighted that sample D1#4 provided the best in detection efficiency, showing a neutron response equal to 0.021 cm^2. A set of new D1 detectors with the same characteristics of the probe #4 was therefore fabricated. A Data AcQuisition system for the processing and acquisition of signals generated by the ATND was developed. In view of the parallel acquisition of multiple detectors, a commercial 8-channel digital oscilloscope, which provides 8 analog inputs, simultaneously sampled at a maximum rate of 2 MS s^{-1} with a resolution of 16 bits, was selected. Digital filtering and spectrum processing were carried out in streaming mode by means of an *ad hoc* developed Labview2010 program, whose purpose was to simultaneously acquire and process pulses provided by eight different detectors.

Preliminary irradiation tests, performed with 5 MeV and 565 keV neutrons, of a low-cost prototype of the cylindrical spectrometer, equipped with the previously developed D1 sensors, confirmed the possibility of simultaneously acquire and elaborate signals from different detectors within a single moderating structure, but also pointed out some criticalities to face, regarding both the discrete acquisition electronics and the

response of the active sensors in mixed fields. In order to overcome these critical aspects, new solutions were proposed. Multiple discrete electronic chains were integrated and parallelized in portable multi-channel boards and a new preliminary study about another ATND, called D2, was performed. Six samples, D2#1-6, which differed in the neutron sensibility, were developed. Irradiations in thermal neutron field established that sample D2#6 provided the best in detection efficiency, showing a neutron response equal to 0.026 cm^2.

The two types of ATND were tested within a standard Extended Range Bonner Sphere Spectrometer System (ERBSS), in order to check their performances for neutron spectrometry. Preliminary data demonstrate the agreement between results derive through the two sensors with respect to a reference ^{6}LiI ATND. Their efficiency resulted about eight times lower than that of the LiI sensor. On the other hand, the great advantage of these new ATND, compared with the scintillator detector, is their very small dimensions and their cheapness.

A final comparison between the D1#4 and D2#6 detectors displayed the following major outcomes:

- the response of the two detectors is similar; in particular, the D2#6 exhibits slightly better performance, being its response equal 0.026 cm^2 *vs.* 0.021 cm^2 for the D1#4;
- the use of the D2 detectors largely enhance the effectiveness of the n-γ discrimination. The spectra obtained by means of the D2 show a net separation between gamma and neutron contribution. A proper threshold is sufficient to derive counts due to neutrons;
- the D1 sensor main advantage of featuring a higher thermal neutron sensibility is balanced (and penalized) by a large photon contribution and a worse signal-to-noise ratio.

For these reasons, the D2 ATND was selected as the best option.

In the next future, these sensors will replace the passive detectors in the final spherical and cylindrical spectrometers proposed in the framework of the NESCOFI@BTF Project. The resulting instruments will be real-time spectrometers able to simultaneously provide all energy components of the neutron field in a single irradiation.

REFERENCES

[1] J. Chadwick, The existence of a neutron, Proceedings of the Royal Society A 136 (1932) 692-708.

[2] K. S. Krane, Introductory Nuclear Physics, John Wiley & Sons, 1988.

[3] J. Turner, Atoms, Radiation and Radiation Protection, 2nd Edition, John Wiley & Sons, 1995.

[4] G.F. Knoll, Radiation Detection and Measurement, Third Edition, John Wiley & Sons, 2000.

[5] F. Brooks, H. Klein, Neutron spectrometry - historical review and present status, Nuclear Instruments and Methods in Physics Research A 476 (476) (2002) 1-11.

[6] D. Thomas, A. Alevra, Bonner sphere spectrometers - a critical review, Nuclear Instruments and Methods in Physics Research A 476 (2002), 12-20.

[7] A. Alevra, D. Thomas, Handbook on neutron and photon spectrometry techniques for radiation protection, Radiation Protection Dosimetry 107 (1-3) (2003), 37-72.

[8] D. Thomas, Radiation Measurements 45 (2010) 1178.

[9] B. Wiegel, A. Alevra, Nuclear Instruments and Methods in Physics Research A 476 (2002) 36.

[10] A. Esposito, R. Bedogni, C. Domingo, M.J. Garcia, K. Amgarou, Radiation Measurements 45 (2010) 1522.

[11] R. Bedogni, D. Bortot, B. Buonomo, M. Chiti, M. De Giorgi, A. Esposito, A. Gentile, J. M. Gomez-Ros, G. Mazzitelli, M.V. Introini, A. Pola, L. Quintieri, NESCOFI@BTF NEutron Spectrometry in COmplex FIelds @ Beam Test Facility, INFN website, Annual Reports 2011.

[12] A. Alevra, D. Thomas, Neutron spectrometry in mixed fields: multisphere spectrometers, Radiation Protection Dosimetry 107 (1-3) (2003) 37-72.

[13] J.M. Gomez-Ros, R. Bedogni, I. Palermo, A. Esposito, A. Delgado, M. Angelone, M. Pillon, Design and validation of a photon insensitive multi detector neutron spectrometer based on Dysprosium activation foils, Radiation Measurements 46-12 (2011).

[14] J. M. Gomez-Ros, R. Bedogni, M. Moraleda, A. Esposito, A. Pola, M.V. Introini, G. Mazzitelli, L. Quintieri, B. Buonomo, Designing an extended energy range single-sphere multi-detector neutron spectrometer, Nuclear Instruments and Methods in Physics Research A 677 (2012) 4-9.